

**CHANGES IN MUSKMELON PERISPERM ENVELOPE TISSUE
DURING GERMINATION**

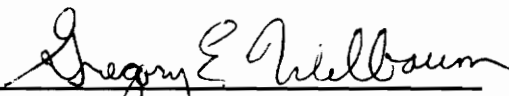
by

Wangechi Muthui

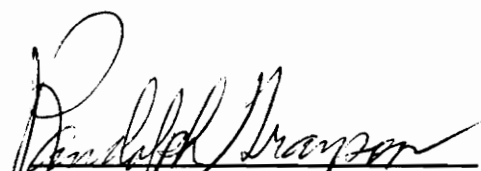
Thesis submitted to the faculty of the
Virginia Polytechnic Institute and State University
in partial fulfillment of the requirements for the degree of
Master of Science
in

Horticulture

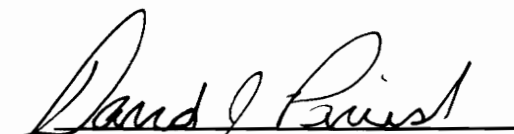
APPROVED:



Gregory Welbaum



Randolph Grayson



David Parrish

August, 1993

Blacksburg, Virginia

C.2

LD
5655
V855
1993
M879
C.2

Changes in muskmelon perisperm envelope during germination

by

Wangechi Muthui,

Gregory Welbaum, Chairman

Horticulture

(ABSTRACT)

Muskmelon (*Cucumis melo* L.) embryos are surrounded by a single layer of endosperm and a two- to four-cell-layered perisperm. The embryonic axis must penetrate the perisperm envelope (perisperm + endosperm) for germination to occur. Radicle emergence could result from increased turgor, weakening of the perisperm tissue, or a combination of both. In a previous report, turgor of the embryonic axis did not increase prior to radicle emergence. This suggests that weakening of the perisperm envelope is a prerequisite for radicle emergence in muskmelon seeds. The changes in cell wall sugars of the perisperm tissue were studied during imbibition using gas chromatography and high performance thin layer chromatography. The major cell wall sugars identified in the micropylar perisperm tissue were glucose, galactose, xylose, and rhamnose. Endo- β -mannanase has been shown to be responsible for endosperm degradation in seeds of Solanaceae, Leguminosae, and Fabaceae. However, the lack of mannose in the cell walls of muskmelon perisperm tissue suggests that this enzyme is not involved in muskmelon seed germination. Structural changes of the micropylar perisperm envelope tissue were visualized during imbibition using electron microscopy. Scanning electron microscope images revealed changes in the perisperm envelope

before radicle protrusion. The cell walls of the perisperm envelope tissue were degraded starting 5 h prior to radicle emergence. An Instron was used to measure the mechanical resistance of the perisperm envelope during imbibition. The force and total energy required to penetrate the perisperm tissue of imbibed muskmelon seeds decreased gradually during imbibition. This study confirmed that the perisperm envelope tissue offered mechanical resistance to the expanding embryonic axis. Degradation of the perisperm envelope tissue before radicle protrusion facilitated radicle emergence.

ACKNOWLEDGMENTS

This project would not be without the help and encouragement from Dr. Gregory Welbaum. I thank Dr. Richard Fell and Keith Tignor for their help with the sugar analysis, Dr. Wilson and Donnie for their help with the Instron work, and Dr Grayson, Ginny Viers and Kathy for their assistance with the electron microscopy work. In addition, for his advice and serving on my Committee, I thank Dr. David Parrish.

Finally but not least importantly, I thank my family; Wambui, Wanjiru, Wairimu, Gachigi, and Bachia for their constant support and encouragement throughout the years. Thank you very much for your special letters. In addition, I have no words to express my sincere gratitude to Nyambura, Agnes, Shaban, and Mike; you are wonderful people.

DEDICATION

Muthoni and Muthui

TABLE OF CONTENTS

| | |
|---|--------|
| ABSTRACT..... | ii |
| ACKNOWLEDGEMENTS..... | iv |
| DEDICATION..... | v |
| LIST OF TABLES | viii |
| LIST OF FIGURES..... | ix |
| CHAPTER ONE | 1 |
| LITERATURE REVIEW | 1 |
| Seed types..... | 1 |
| Germination process..... | 2 |
| Mechanism of radicle emergence..... | 3 |
| Biochemical aspects of the endosperm..... | 6 |
| Muskmelon seeds..... | 9 |
| CHAPTER TWO | 10 |
| STRUCTURAL CHANGES IN MUSKMELON PERISPERM ENVELOPE TISSUE DURING GERMINATION | 10 |
| INTRODUCTION | 10 |
| Scanning electron microscopy | 15 |
| MATERIALS AND METHODS..... | 16 |
| Plant material | 16 |
| Processing..... | 16 |
| Fresh samples..... | 19 |
| Photography | 19 |
| RESULTS AND DISCUSSION..... | 20 |
| CHAPTER THREE..... | 46 |
| CHANGES IN CELL WALL SUGARS OF MUSKMELON PERISPERM TISSUE DURING IMBIBITION | 46 |
| INTRODUCTION | 46 |
| Chromatography..... | 50 |
| MATERIALS AND METHODS..... | 53 |
| Plant material | 53 |

| | |
|---|-----|
| Time-course for germination..... | 53 |
| Incubation conditions | 53 |
| Extraction of cell walls | 54 |
| Gas chromatography..... | 54 |
| Sugar standard..... | 54 |
| Trimethylsilyl derivation of cell wall sugars: TMS Ethers of Methyl Glycosides | 55 |
| Quantitative analysis | 56 |
| High Performance Thin Layer Chromatography | 57 |
| Sugar standard..... | 57 |
| HCl in methanol hydrolysis | 57 |
| Trifluoroacetic acid (TFA) hydrolysis | 57 |
| HPTLC plates | 58 |
| Solvents | 58 |
| Sample application and development | 59 |
| Visualization | 60 |
| Quantitative analysis | 60 |
| RESULTS AND DISCUSSION | 61 |
| CHAPTER FOUR..... | 75 |
| CHANGES IN THE STRENGTH OF PERISPERM TISSUE DURING MUSKMELON SEED GERMINATION | 75 |
| INTRODUCTION | 75 |
| MATERIALS AND METHODS..... | 79 |
| Plant material | 79 |
| Incubation conditions | 79 |
| Puncture-test | 79 |
| Crosshead speed test | 80 |
| Quantification..... | 80 |
| RESULTS AND DISCUSSION | 81 |
| SUMMARY..... | 92 |
| LITERATURE CITED..... | 95 |
| VITA | 104 |

LIST OF TABLES

| | | |
|-------------|--|----|
| Table: 3.1. | Sugar standards developed in propanol:water. (90:10). Visualization: thymol-sulfuric acid reagent. | 66 |
| Table: 3.2. | Monosaccharide concentrations ($\mu\text{g mg}^{-1}$ dry weight) in cell walls of muskmelon perisperm tissue cone tips determined by HPTLC. | 71 |
| Table: 3.3. | Monosaccharide concentrations ($\mu\text{g mg}^{-1}$ dry weight) in cell walls of muskmelon perisperm tissue without cone tips determined by HPTLC. | 71 |
| Table: 3.4. | Monosaccharide concentrations ($\mu\text{g mg}^{-1}$ dry weight) in cell walls of intact muskmelon perisperm tissue determined by HPTLC. | 71 |

LIST OF FIGURES

| | | |
|-----------|---|----|
| Fig. 2.1. | Germination time-course of muskmelon seeds at 25°C. Germination was defined as radicle emergence from the perisperm envelope tissue. | 21 |
| Fig. 2.2. | Processed micropylar muskmelon perisperm envelope tissues at 10 h. A) The smooth outer layers are perisperm (P). B) The inner layer is endosperm (E). The outer perisperm tissue is covered with tissues from the testae. | 23 |
| Fig. 2.3. | Micropylar muskmelon perisperm envelope tissues adjacent to the radicle. There is no apparent degradation of the endosperm tissue at 10 h. A) Processed. B) Fresh-coated. | 26 |
| Fig 2.4. | Micropylar muskmelon perisperm envelope tissues adjacent to the radicle at 15 h. The endosperm (E) tissue adjacent to the radicle tip is visible. A) Processed. B) Fresh-coated. | 28 |
| Fig. 2.5. | Micropylar muskmelon perisperm envelope tissues adjacent to the radicle at 15 h. There is no apparent degradation. A) Processed. B) Fresh-coated. | 30 |
| Fig. 2.6. | Micropylar muskmelon perisperm envelope tissues adjacent to the radicle at 20 h. Arrow shows a crack between adjacent cells. A) Processed. B) Fresh-coated. | 32 |
| Fig. 2.7. | Micropylar muskmelon perisperm envelope tissues adjacent to the radicle at 25 h. A) The cracks are more severe. B) Part of the wall is broken. Arrows show cracks. | 35 |

| | | |
|------------|---|----|
| Fig. 2.8. | Micropylar muskmelon perisperm envelope tissues adjacent to the radicle at 30 h. A) Radicle emergence has occurred as indicated by the large opening. B) The tissue is ruptured by the emerging radicle. Arrows show cracks. | 37 |
| Fig. 2.9. | The tip of a dry, decoated muskmelon seed. The outer layers of the perisperm (P) as well as layers of the testae (T) covering part of the perisperm tissue are visible. | 39 |
| Fig. 2.10. | The tip of a decoated germinating muskmelon seed at 30 h. A) The perisperm tissue is fractured along sides to allow embryo (e) expansion. B) The degraded endosperm (E) is visible. | 41 |
| Fig. 2.11. | Micropylar muskmelon perisperm envelope tissue adjacent to the radicle at 48 h. The endosperm tissue is degraded and cell contents seem to be missing. | 43 |
| Fig. 3.1. | GC recordings of cell wall sugars of muskmelon perisperm cone tips from seeds imbibed for 25 h. Arabinose (1), rhamnose (2), fucose (3), xylose (4), galacturonic acid (5), mannose (6), galactose (7), glucuronic acid (8), glucose (9) and Myo-inositol (internal standard) (10). | 62 |
| Fig. 3.2. | The changes in cell wall sugars of muskmelon perisperm cone tips determined by GC during imbibition. | 63 |
| Fig. 3.3. | The changes in cell wall sugars of muskmelon perisperm cone tips determine by GC during imbibition. | 64 |

| | | |
|-----------|--|----|
| Fig. 3.4 | Scanner recordings of cell wall sugar chromatograms of muskmelon perisperm envelope tissue 25 h after the start of imbibition on silica gel 60 HPTLC developed with two different reagents. A) solvent D (propanol:water, 90:10) gave Glucose (1), galactose (2), xylose (3), rhamnose (4), solvent front (5). B) Solvent A (Ethylacetate:acetic acid:methanol:water, 12:3:3:2) gave Glucose and galactose (1), xylose (2), rhamnose (3), solvent front (4). | 67 |
| Fig. 3.5. | Changes in sugar concentrations determined by HPTLC in the cell walls of muskmelon perisperm cone tips during imbibition. | 68 |
| Fig. 3.6. | Changes in sugar concentrations determined by HPTLC in the cell walls of muskmelon perisperm tissue without cone tips during imbibition. | 69 |
| Fig. 3.7. | Changes in sugar concentrations determined by HPTLC in the cell walls of intact muskmelon perisperm envelope during imbibition. | 70 |
| Fig. 3.8. | Standard curves for rhamnose, xylose and glucose from HPTLC plates developed with propanol:water (90:10). Visualization: Thymol-sulfuric acid reagent. | 72 |
| Fig. 4.1. | Changes in the force needed to penetrate the muskmelon perisperm tissue during imbibition. Radicle emergence was evident at 23 h. | 82 |
| Fig. 4.2. | Changes in the energy needed to penetrate the muskmelon perisperm tissue during imbibition. Radicle emergence was evident at 23 h. | 83 |

| | | |
|-----------|---|----|
| Fig. 4.3. | Changes in pressure of the muskmelon seed tissues at 22 h during penetration. The arrow shows the peak (maximum load) and the cross-hatch shows the total energy. | 84 |
| Fig. 4.4. | Changes in pressure of the muskmelon seed tissues at 25 h during penetration. The arrow shows the peak (maximum load) and the cross-hatch shows the total energy. | 85 |
| Fig. 4.5. | Changes in the energy required to penetrate the muskmelon perisperm envelope tissue using three crosshead speeds. | 87 |
| Fig. 4.6. | Changes in the force required to penetrate the muskmelon perisperm envelope tissue using three crosshead speeds. | 88 |

CHAPTER ONE

LITERATURE REVIEW

Seed types

A seed is a miniature plant in an arrested state with food reserves to sustain the young plant until a self-sufficient, autotrophic organism can be established. One category of seeds is based on the presence or absence of maternal tissue. The embryos of rapeseed (*Brassica napus*), and mustard (*Sinapsis alba*), for instance, are not surrounded by layers of tissue (Schopfer *et al.* 1979, Schopfer and Plachy 1984, 1985). The testa in these seeds, does not represent a mechanical barrier to the radicle, because it is thin, fragile, and cracks open during imbibition.

In other species, such as lettuce (*Lactuca sativa*), (*Datura stramonium*), tomato (*Lycopersicon esculentum*), pepper (*Capsicum annum*), and muskmelon (*Cucumis melo*), the embryonic axis is completely surrounded by layers of endosperm, perisperm, or other heterogeneous tissues that may restrict radicle growth (Georghiou *et al.* 1983, Watkins *et al.* 1985, Groot and Karssen 1987, Sanchez *et al.* 1990, Welbaum and Bradford 1990a). The germination process in such seeds is complicated, because the embryonic axis must penetrate tissues that do not open during imbibition (Bradford 1990, Ni and Bradford 1992). The changes in morphology of tomato, *Datura*, lettuce, and pepper endosperm during imbibition have been previously described (Jones 1974, Pavlista and Valdovinos 1978, Psaras *et*

al. 1981, Georghiou *et al.* 1983, Psaras 1983, Watkins *et al.* 1985, Groot and Karssen 1987, Haigh and Barlow 1988, Sanchez *et al.* 1990).

Germination process

Seed germination is the process of initiating growth of a previously quiescent or dormant embryo. For most seeds, germination begins with imbibition and ends with radicle emergence. Generally, imbibition is a triphasic process (Bewley and Black 1978, Weges 1987, Haigh and Barlow 1987, Bradford 1990). Phase I is characterized by rapid water uptake. Phase I is followed by a plateau, equilibrium or lag phase (Phase II), with little change in water content. Phase III is concurrent with radicle elongation and is accompanied by an increase in water uptake. Phase II is generally the longest of the three phases, and many metabolic activities take place in preparation for radicle emergence. Phase II is of considerable interest, because factors that control germination rate influence the duration of this phase. Seed dormancy can be extended by extreme temperatures, water stress, or abscisic acid, while factors that promote germination do so by shortening the lag phase. Once the radicle has penetrated enclosing tissues and is growing, germination is complete and seedling growth has begun (Bradford 1990).

In some seeds that lack maternal tissue such as rapeseed, the germination process is characterized by an initial imbibition phase followed immediately by a growth phase (Schopfer and Plachy 1984, 1985). The radicle must penetrate perisperm or endosperm tissues in order for

germination to occur in seeds with maternal tissues (Bradford 1990, Ni and Bradford 1992). In such seeds, the length of phase II may be directly related to the rate of degradation of these tissues (Bradford 1992). In tomato, pepper, and muskmelon, removal of the barrier imposed by the envelope tissues greatly accelerates radicle growth (Watkins and Cantliffe 1985, Bradford and Dahal 1990, Welbaum and Bradford 1990a, 1990b).

Mechanism of radicle emergence

Several strategies that the embryo could employ to penetrate surrounding tissues have been proposed. Enzymatic or mechanical weakening of surrounding tissues would free the expanding embryo from restraint (Jones 1974, Georghiou *et al.* 1981, Liptay and Schopfer 1983, Groot and Karssen 1987, Sanchez *et al.* 1990, Welbaum and Bradford 1990b). Embryo expansion and radicle growth could be accomplished by an increased ability of the embryo to take-up water, weakening of the restraining tissue, or a combination of both (Welbaum and Bradford 1990a). Reduction in mechanical strength could result from mechanical force of the growing embryo pushing against the restraining tissue, or from enzymatic degradation of the barriers until they no longer constitute a barrier to radicle emergence (Welbaum and Bradford 1990b).

Embryos could overcome the restraint of the barrier by generating additional hydrostatic pressure by accumulating osmotic solutes (Carpita *et al.* 1979a, Takeba 1980, Bradford 1986). This would allow radicles to simply burst through the barrier tissue when sufficient hydrostatic pressure

was generated. The ability of seeds to germinate at lower water potentials is increased by factors that stimulate seed germination such as light and growth regulators (Nabors and Lang 1971a, 1971b, Carpita *et al.* 1979a, 1979b, Thanos 1984). This increased growth potential has been attributed, in part, to solute accumulation (Carpita *et al.* 1979a, 1979b, Thanos 1984). In lettuce and watermelon, direct measurements of solute potential in excised axes have failed to account completely for the increased growth potentials observed (Carpita *et al.* 1979a, 1979b, Thanos 1984), indicating that decreased yield threshold or increased cell wall extensibility may be responsible for radicle growth during germination.

Turgor undoubtedly plays an important role in the germination process as predicted by the Lockhart model for expansive growth (Lockhart 1965, Bradford 1990). Increase in embryo turgor due to water uptake accelerates endosperm weakening, thus enhancing the rate of germination. In lettuce, there is conflicting evidence about the relative importance of endosperm weakening in the germination process (Nabors and Lang 1971a, 1971b, Jones 1974, Carpita *et al.* 1979a, 1979b, Georghiou *et al.* 1981, 1983, Bradford 1990). Some reports suggest changes in turgor or growth potential are the key to radicle emergence. However, direct measurements of turgor in lettuce radicles just prior to germination do not support these claims (Weges 1987, Bradford 1990). Thermodynamic evidence predicts that lettuce seed germination occurs because of mechanical weakening of the endosperm and not an increase in embryo turgor (Weges 1987, Bradford 1990). Red-light stimulates lettuce seed germination by changing the balance between growth potential of the embryo and the resistance from the surrounding tissues

(Carpita *et al.* 1979a, Bewley and Black 1982). Evidence suggests that endosperm weakening and not increased turgor, is a prerequisite for radicle emergence in tomato and pepper, (Watkins and Cantliffe 1983, Watkins *et al.* 1985, Haigh and Barlow 1987, Groot *et al.* 1988). In *Datura*, evidence suggests that increase in turgor and endosperm weakening both precede radicle emergence (Sanchez and De Miguel 1985, Sanchez *et al.* 1990). Many of these studies have focused on changes on growth potential of seeds incubated in osmotic solutions (Groot *et al.* 1988, Sanchez *et al.* 1990). Red-light enhances mechanical weakening of *Datura ferox* endosperm by stimulating embryo growth potential (Sanchez and De Miguel 1985, Sanchez *et al.* 1990). Radicle growth in rapeseed is correlated with an increase in growth potential due to water uptake by the embryo (Schopfer and Plachy, 1985). During rapeseed germination, turgor yield threshold decreases, while embryo cell wall extensibility increases without significant changes in solute accumulation or hydraulic conductivity.

Enzyme-induced weakening of tissues surrounding the embryo is a possible mechanism of radicle emergence (Ikuma and Thimann 1963, Pavlista and Valdovinos 1971, Groot and Karssen 1987, 1988, Welbaum and Bradford 1990a). Barriers to radicle emergence could be degraded until they no longer constitute a significant hindrance (Welbaum and Bradford 1990a). Enzyme degradation of tissues surrounding the embryo could control germination in many species by reducing the turgor threshold necessary for expansive growth of the radicle (Bradford 1990).

Growth regulators influence radicle emergence in seeds such as tomato and pepper (Liptay and Schopfer 1983, Groot and Karssen 1987a, 1987b

Watkins *et al.* 1985). The use of abscisic acid and a gibberellin-deficient mutants in tomato enabled Groot *et al.* (1988) to block germination and to restore the ability to germinate by addition of gibberellins. Evidence suggested that weakening of endosperm cells around the radicle tip prior to emergence in tomato and pepper is mediated by growth regulators (Watkins and Cantliffe 1985, Groot and Karssen 1987, Groot *et al.* 1988). Absciscic acid inhibits germination in these seeds by blocking gibberellin-induced weakening of the endosperm (Groot and Karssen 1987), thus preventing the embryo from overcoming the opposing force of the seed layers covering the radicle tip (Liptay and Schopfer 1983). In mustard seeds, ABA inhibits embryo water uptake by preventing cell wall loosening, thus delaying germination (Schopfer and Plachy 1985).

Biochemical aspects of the endosperm

Both the cotyledons and the endosperm may provide a source of carbohydrate during germination. In some species, the cell wall of the endosperm becomes thickened at seed maturity and apparently serves as a carbohydrate reserve. Increased cell wall thickening is sometimes associated with deposition of one type of polysaccharide with specific sugar composition and bond linkage patterns. The linear main backbone chains are composed of one or sometimes two sugars, which are usually β -linked. Attached to the main chain are greater or lesser numbers of short side chains usually α -linked, often one to three residues long, which contain sugars different from the main chain (Halmer 1985).

Most carbohydrates based upon (1→4)-β-mannans are used as food reserves in seeds of several monocot and dicot genera (Meier and Reid 1971). In legumes, such as fenugreek (*Trigonella foenum-graecum*), carob (*Ceratonia siliqua*), and guar (*Cyamopsis tetragonoloba*) galactomannans [long-chain (1→4)-β-mannan backbone chains substituted with single (1→6)-α-galactose side chains] are stored in the thick cell walls of the endosperm (Reid 1971, McCleary and Matheson 1974, Seiler 1977). Endosperm mobilization depends upon the production of endo-β-mannanase, exo-β-mannanase (β-mannosidase), and α-galactosidase enzymes that are secreted by the living cells of the endosperm (Meier and Reid 1982, Reid 1985). The key hydrolyzing enzyme in these seeds is endo-β-mannanase (Meier and Reid 1975).

The lettuce endosperm consists of two layers of cells with thick walls containing 60% mannose, presumably (1→4)-β-mannan (Halmer *et al.* 1975) based on higher plants (Black and Chapman 1990). Halmer *et al.* (1976) found that mannanase activity in lettuce endosperm was responsible for the retrieval of storage reserve mobilization, but the relationship between mannanase activity and endosperm weakening was not investigated. In cv. Grand Rapids, the endosperm is completely mobilized as a food reserve before the main embryonic reserves are depleted (Halmer *et al.* 1978, Leung *et al.* 1979). The process is accompanied by production of endo-β-mannanase in the endosperm and β-mannosidase in the cotyledons (Halmer and Bewley 1979, Leung *et al.* 1979). Although mannanase activity is high in lettuce endosperm tissue, it is unclear whether its activity is linked to radicle emergence in these seeds (Halmer and Bewley 1979). Biochemical changes

in lettuce achenes stimulated to germinate by red-light or gibberellin application occur mostly after radicle protrusion (Halmer *et al.* 1976, Carpita *et al.* 1979a, 1979b, Bewley and Halmer 1980, 1981, Leung and Bewley 1981). Endo-(1→4)-β-mannanase produced in endosperms of lettuce achenes breaks the mannose-based carbohydrates of the cell wall early after radicle emergence (Halmer *et al.* 1975, Dulson *et al.* 1988). Alpha-galactosidase is the only enzyme that is clearly enhanced before radicle emergence in lettuce seeds (Leung and Bewley 1981).

In seeds of the solanaceous family such as *Datura*, tomato, and pepper, endosperm cell wall composition may be similar. In *Datura*, the endosperm cell walls are composed of 4-linked mannan. The timing of mannan loss from the endosperm wall in *Datura* occurs prior to radicle emergence, following phytochrome induction to germinate (Sanchez *et al.* 1990). The endosperm cell walls in tomato, and possibly pepper, are mainly composed of mannan or galactomannan (Watkins and Cantliffe 1985, Groot *et al.* 1988). Endo-β-mannanase activity in *Datura* and tomato is correlated with release of mannose and endosperm weakening (Groot *et al.* 1988).

In albuminous seeds such as celery (*Apium graveolens*), the living endosperm consists mostly of large angular thick-walled cells containing aleurone grains and lipid droplets. Hydrolases released from the endosperm are thought to be responsible for endosperm breakdown in response to gibberellin released from the embryo (Jacobsen *et al.* 1976).

Other cell wall polysaccharides found in the endosperm or cotyledons of seeds include arabino-(1→4)-β-xylan and (1→4), (1→3)-β-glucan in cell walls of cereal endosperms. Xylo-(1→3)-β-glucans occur in the endosperm

of *Tamarindus indica* (Matheson and Saini 1977). Galacto-xylo-(1→4)- β -glucan has been identified in endosperms of seven dicot families (Courtois *et al.* 1976).

Muskmelon seeds

Muskmelon seed germination is slow with seeds remaining in phase II for an extended period. This delay is especially significant at low temperatures; the lag phase can last up to 7 d at 15°C. Germination studies of embryos without the perisperm show a significant increase in germination rate. Radicle growth is possibly allowed by weakening of the perisperm envelope surrounding muskmelon embryos, because no significant changes in embryo turgor occur during imbibition (Welbaum and Bradford 1990a). In the current study, changes in cell wall composition of muskmelon perisperm envelope were investigated during various stages of imbibition using gas and high performance thin-layer chromatography. Structural changes of the perisperm tissue were examined using scanning electron microscopy, while forces needed to penetrate the perisperm envelope during imbibition were quantified using an Instron. The results presented in the current study illustrate the role of the perisperm envelope in regulating muskmelon seed germination.

CHAPTER TWO

STRUCTURAL CHANGES IN MUSKMELON PERISPERM ENVELOPE TISSUE DURING GERMINATION

INTRODUCTION

Seed germination is the process of initiating growth of a previously quiescent or dormant embryo. For most seeds, germination begins with imbibition and ends with radicle emergence. In seeds of lettuce, *Datura*, tomato, pepper, and muskmelon, the embryo is surrounded by endosperm, perisperm, or other heterogeneous tissues that may restrict radicle growth (Georghiou *et al.* 1983, Watkins *et al.* 1985, Sanchez *et al.* 1990, Welbaum and Bradford 1990a). In such seeds, imbibition is triphasic (Bewley and Black 1982, Haigh and Barlow 1987, Weges 1987, Bradford 1990). Phase I is characterized by rapid water uptake followed by little change in water content during phase II, when many metabolic processes occur in the seed, in preparation for radicle emergence. Phase III is concurrent with radicle elongation and is accompanied by an increase in water uptake. Once the radicle has penetrated enclosing tissues and is growing, germination is complete and seedling growth has begun (Bradford 1990).

In seeds that have maternal tissue surrounding the embryo, the radicle may have to overcome the force of the restraining tissue during germination. The exact role of the endosperm and the mechanism of its rupture are still poorly understood (Ikuma and Thimann 1963, Evenari 1965, Mayer and

Shain 1974). Several authors have studied the lettuce endosperm intensively to determine the exact role of this tissue in restricting radicle protrusion (Pavlista and Harber 1970, Halmer and Bewley 1975, Halmer *et al.* 1975, 1976). In lettuce seeds, for example, germination rate was enhanced by surgically removing or puncturing the lettuce endosperm (Ikuma and Thimann 1963, Speer 1974). Evidence suggests that the mechanical force of the growing embryo as well as enzymatic weakening of the endosperm is necessary for germination in tomato (Groot and Karssen 1987, Haigh and Barlow 1987, Bradford 1990, Dahal and Bradford 1990). The morphology of tissues surrounding the embryo has been studied in seeds of lettuce, tomato, pepper, *Datura*, and muskmelon (Jones 1974, Pavlista and Valdovinos 1978, Georgiou *et al.* 1983; Psaras *et al.* 1983, Watkins *et al.* 1985, Haigh *et al.* 1990, Sanchez *et al.* 1990, Welbaum and Bradford 1990a). The similarity between the degradative changes occurring in the cereal aleurone layer and the dicot endosperm has also been recognized (Jacobsen 1984).

Biochemical changes of the endosperm cell wall have been studied during imbibition (Halmer and Bewley 1975, Halmer *et al.* 1975, 1976, Groot and Karssen 1988, Sanchez *et al.* 1990). The major cell wall component of the endosperm in lettuce, tomato, *Datura*, and possibly pepper is mannan. The major biochemical events in lettuce endosperm cells, such as mobilization of endosperm-stored reserves and endosperm cell wall breakdown, occur mostly after radicle emergence (Halmer *et al.* 1978, Halmer and Bewley 1979, Bewley and Halmer, 1980, 1981).

There is evidence that structural changes take place in lettuce endosperm during germination (Jones 1974, Pavlista and Valdovinos 1978,

Psaras *et al.* 1981, Georghiou *et al.* 1983, Psaras 1983). The lettuce embryo is surrounded by a two- to four- cell layered endosperm tissue in the micropylar region. Jones (1974) observed changes in the endosperm cells and cell walls using light microscopy and attributed the cross-sectional structure of the endosperm to the role of endosperm in restricting radicle emergence during germination. Scanning electron microscopy (SEM) studies revealed weakening of the entire lettuce endosperm cell walls prior to onset of germination (Jones 1974). In other studies, evidence suggests that structural alterations of lettuce endosperm cells occurred exclusively at the micropylar end. Previous findings by Jones (1974) possibly were based on germinated seeds (Psaras *et al.* 1981, Georghiou *et al.* 1983, Psaras and Georghiou 1983). Endosperm cells of dark-germinating Grand Rapids lettuce undergo significant structural changes at the radicle tip prior to radicle emergence (Georghiou *et al.* 1983). Similarly, phytochrome activity (Psaras *et al.* 1981) and gibberellin application (Psaras and Georghiou 1983) induce pre-emergence changes in micropylar endosperm cells of light-requiring Grand Rapids lettuce achenes. Using electron microscopy, Pavlista and Valdovinos (1978) observed cracks and pits on the surface of the micropylar endosperm prior to radicle emergence in light-requiring lettuce. Such pre-emergence changes were absent in light-requiring lettuce seeds imbibed in non-inducing conditions including far-red light, darkness, and extreme temperatures (Jones 1974, Pavlista and Valdovinos 1978). The authors concluded that localized structural changes of the endosperm were a key event during lettuce seed germination.

In tomato, radicle growth is restricted by an endosperm that surrounds the embryo (Liptay and Schopher 1982, Haigh and Barlow 1987, Groot *et al.* 1988). The morphology of tomato endosperm in wild-type and mutant seeds has been studied using light and electron microscopy (Groot and Karssen 1987, Haigh and Barlow 1988, Haigh *et al.* 1992). Haigh and Barlow (1987) identified a region of smaller, thin-walled cells in tomato endosperm immediately opposite the radicle tip that appeared to separate coincident with radicle growth. Haigh and coworkers (1990) confirmed that the tomato endosperm consisted of two identifiable cell types found in separate locations of the tissue. At the micropylar end of the seed (surrounding the radicle), the endosperm cells had thin walls, whereas, lateral cells had thicker walls. They observed alterations in the endosperm cells of the micropylar region during germination, but such changes were absent in the thick-walled endosperm cells. Structural modifications of the endosperm tissue at the micropylar end are a prerequisite for tomato seed germination.

The pepper endosperm restricts embryo expansion during germination. Using electron and light microscopy, Watkins and coworkers (1985) revealed that pepper endosperm tissue directly opposite the radicle tip consisted of seven to nine cell layers. Changes in external appearance of the endosperm directly in front of the radicle tip were characterized by endosperm enlargement, breakdown and loss of cellular integrity, and reduction in tissue thickness one day prior to radicle emergence. The sequence of events observed at the micropylar end led to mechanical weakening and radicle emergence in pepper seeds.

Degradation of *Datura* endosperm is a prerequisite for radicle emergence. Electron microscopy studies revealed that *Datura* endosperm consisted of five to six cell layers at the micropylar end in both *Datura ferox* and *Datura stramonium* (Sanchez *et al.* 1990). Red-light caused degradation and weakening of the endosperm, allowing radicle emergence to occur.

The perisperm envelope in muskmelon seeds offers mechanical resistance to the expanding embryo during imbibition (Welbaum and Bradford 1990a). The muskmelon perisperm envelope consists of a two- to four-cell-layered perisperm and a single-cell-layered endosperm. An anatomical investigation of the perisperm tissue adjacent to the radicle tip revealed an area of smaller cells that were possibly degraded during germination. In these seeds, perisperm degradation appears to be a key event in germination, since there was no evidence of increased turgor in the embryonic axis during germination (Welbaum and Bradford 1990b).

The focus of the current study is to describe structural changes that take place at the micropylar end of muskmelon perisperm envelope before and after radicle protrusion. In this study, the muskmelon micropylar perisperm tissue was visually observed using scanning electron microscopy (SEM). The results from this study will help us understand the role of the perisperm envelope and mechanism of radicle protrusion in germinating muskmelon seeds.

Scanning electron microscopy

The SEM can greatly enlarge three dimensional features of individual cells and whole organisms. The lenses in SEM are used to generate a demagnified, focused spot of electrons that is scanned over the surface of an electrically conductive specimen. As these impinging electrons strike the surface of the specimen, they give rise to signals, including low energy secondary electrons from the uppermost layers of the specimen. Some of the secondary electrons are collected, processed, and eventually translated as a series of pixels on a cathode ray tube or monitor. The brightness of the pixel is directly proportional to the number of secondary electrons generated from the specimen surface. The high resolution obtained and also depth of the image made the SEM a useful optical tool in this study.

MATERIALS AND METHODS

Plant material

Muskmelon cv. Top Mark seeds were obtained from fruits harvested 50 days after anthesis. Twenty seeds were incubated in 9 cm petri dishes on two thickness of germination blotter paper (Anchor Paper Co.) moistened with 10 ml of distilled water. Seeds were incubated at 25°C for 10, 15, 20, 25, 30, and 48 hrs. At the end of each incubation period, seeds were frozen in liquid nitrogen to arrest germination uniformly and to facilitate removal of the perisperm tissue. After removing the seed coat, the seeds were processed whole or dissected to isolate approximately 0.5 mm of the micropylar perisperm tissue (cone tips).

Processing

Fixation was performed overnight (18 hr) in 5% glutaraldehyde in 100 mM sodium phosphate (pH 7.0). Glutaraldehyde is a five-carbon compound containing terminal aldehyde groups which cross-link protein allowing the molecules to bind to lipids, carbohydrates, and nucleic acids. The rate of penetration of glutaraldehyde can be as slow as 1 mm h⁻¹ depending on the type of tissue. The role of the buffering system, used with the primary fixative, was to maintain the physiological pH of the sample to minimize formation of artifacts.

After three buffer rinses of 30 min each, and an additional rinse for 18 h, post fixation was performed using 2% osmium tetroxide for two h. Osmium tetroxide works as a secondary fixative of tissue structure by reacting primarily with lipid moieties. Osmium reacts with the unsaturated fatty acid bonds and is reduced to a dark metallic compound that adds density and contrast to the tissue.

To minimize tissue shrinkage during drying, the samples were dehydrated using a graded ethanol series. The dehydration process involved replacement of water in the cells with a volatile solvent that could evaporate easily with minimum tissue shrinkage. The ethanol series consisted of several changes of 15, 25, 40, and 50% ethanol (20 min) and an overnight change in 75% ethanol. On the second day, sample dehydration was accomplished using 85, 90, and 95% ethanol for 30 min each. Finally, the samples were fully dehydrated using several changes of 100% ethanol for 30 min each.

The dehydrated samples were dried using a critical point drier (Bomar). The samples were placed in EM baskets and transferred into the dehydrant-filled, cooled bomb of the drier. After sealing the vessel, displacement of ethanol in the samples was achieved by using liquid carbon dioxide as a transitional solvent. After several changes of the transitional fluid to ensure complete displacement of the dehydrant, the bomb was completely sealed. The temperature of the transitional fluid was raised slowly. Pressure inside the vessel increased in response to the increased temperature. Eventually, the transitional fluid reached a critical point; a particular pressure/temperature combination (1300 psi/41°C) specific for liquid carbon dioxide. At the critical point, a transition occurred, where the density of the liquid phase

equaled that of the vapor phase, and the samples were fully immersed in a dense vapor phase devoid of the damaging liquid/air interface. The critical temperature was maintained to prevent condensation of the vapor back to liquid, while the vapor was slowly released from the chamber until equilibration with atmospheric pressure was achieved. The procedure described above was fast and reliable. The dried samples were stored in a desiccator to prevent moisture uptake.

The dried perisperm cone tips were mounted on 45° angle aluminum stubs, while whole seeds were mounted on flat stubs. A small amount of adhesive was deposited onto SEM stubs using adhesive transfer tabs. The adhesive, in combination with silver conductive paint, adequately held the specimens firmly on the stubs without causing damage.

To enhance contrast and conductivity, samples were coated with a thin layer (20 to 40 nm) of a conductive gold/palladium alloy using the sputter coating procedure (Hummer X). The specimen stubs were transferred to the specimen chamber that was evacuated (0.1 Pa) to remove any water or oxygen molecules that would damage the surface of the specimen, and argon was slowly introduced into the chamber. A negatively charged, high voltage (3kV) was applied to ionize the argon gas molecules into Ar^+ . The target composed of gold/palladium alloy was bombarded with Ar^+ , that resulted in atoms being ejected from the target. The atoms were deflected by various ions (Ar^+ and electrons) in random pathways to uniformly coat the irregularly shaped specimen surfaces. The metal coatings prevented buildup of high voltage charges on the specimen by conducting excess charges to the ground.

and also provided excellent sources of secondary electrons during observation. The samples were viewed with SEM (Phillips 505).

Fresh samples

After removing the seed coat, approximately 5 mm micropylar perisperm tissue were mounted and coated using the procedure described above.

Photography

The SEM images were recorded by photographing the image off a high resolution cathode ray tube. A camera loaded with 35 mm Polaroid Type 55 instant film was used to record the images. This type of film produced both a high quality negative and a positive print simultaneously. The negative was placed in a concentrated solution of sodium sulfite to remove the developer gel. After 10 s, the negative was washed in running tap water and dipped in a dilute wetting agent (Photo Flo) and dried in a dust-free environment. The positive print was immediately coated with an acidic polymer to neutralize the developer and to seal the print in a plastic layer.

RESULTS AND DISCUSSION

Radicle protrusion usually occurred between 25 and 40 h in most seeds (Fig. 2.1). The SEM images for the fresh-coated and processed samples were similar. However, one advantage of fresh-coated samples over processed samples was that fresh samples were easier to prepare. During viewing, the inner surfaces of most processed cone tips were not visible, because the cut-edges sealed together during processing, while fresh-coated ones were fully open (Fig. 2.2). The SEM images from all imbibition time periods confirmed that, prior to radicle emergence, the radicle tip was completely covered by a perisperm envelope cone tip. A similar cone-shaped structure enclosing the embryo was reported in two *Datura* species (Sanchez *et al.* 1990). The outer surfaces of the cones were rough in appearance; and, in some cases, remains from the seed coats were evident (Fig. 2.2). The layer of material covering the outer surface of the cones had no specific cellular structure and consisted of two layers of cells separated by air spaces when viewed in transverse section. Using light microscopy, Welbaum and Bradford (1990a) described the perisperm tissue as the material that covered the outer surface of the perisperm envelope in muskmelon seeds, and that this tissue consisted of two to four cell layers with no distinctive cellular structure when viewed in cross-section.

On the other hand, the internal surface of the perisperm envelope, that in contact with the embryo, was essentially a smooth sheet composed of rectangular-shaped cells that constituted the residual endosperm tissue (Welbaum and Bradford 1990a).

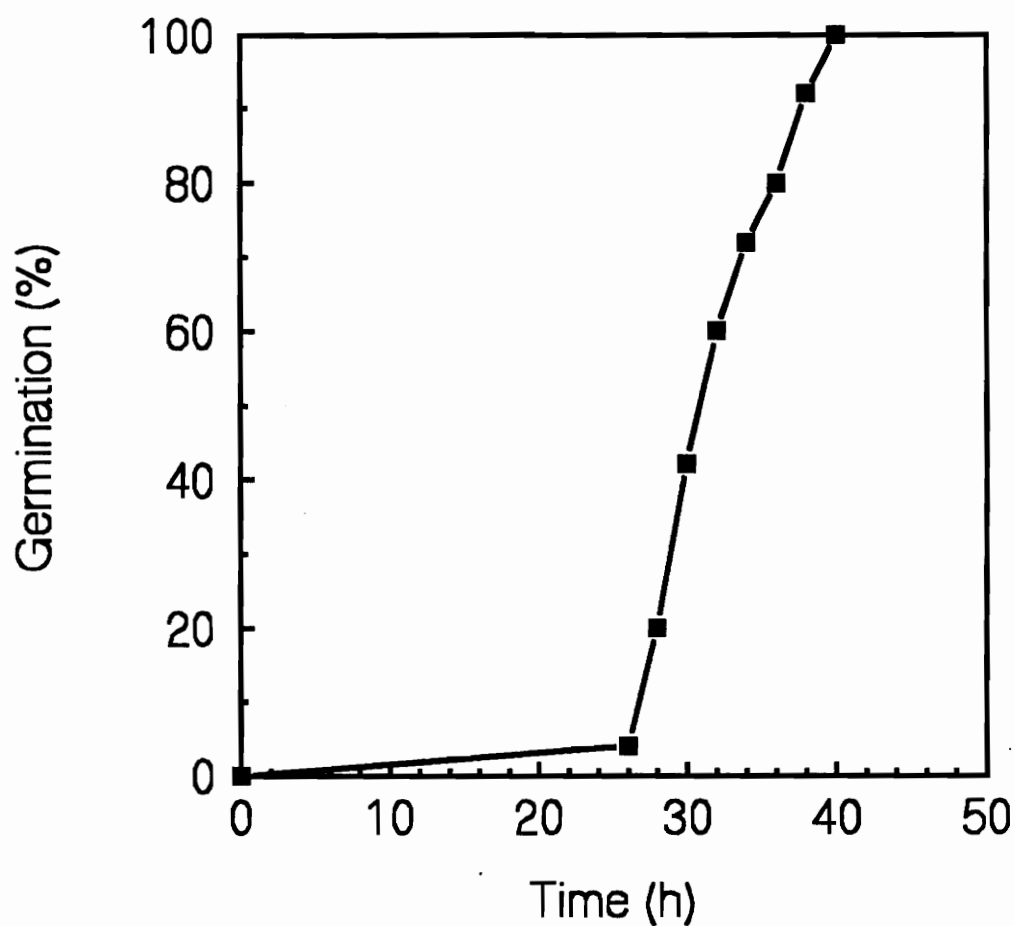
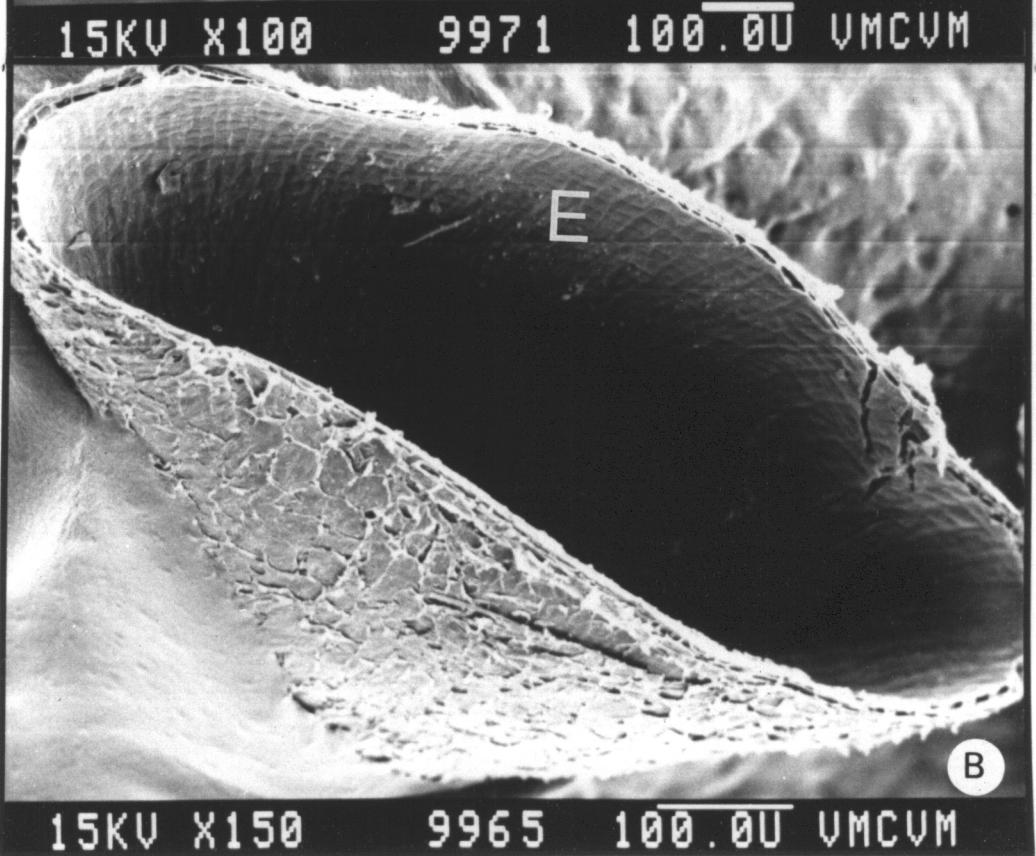
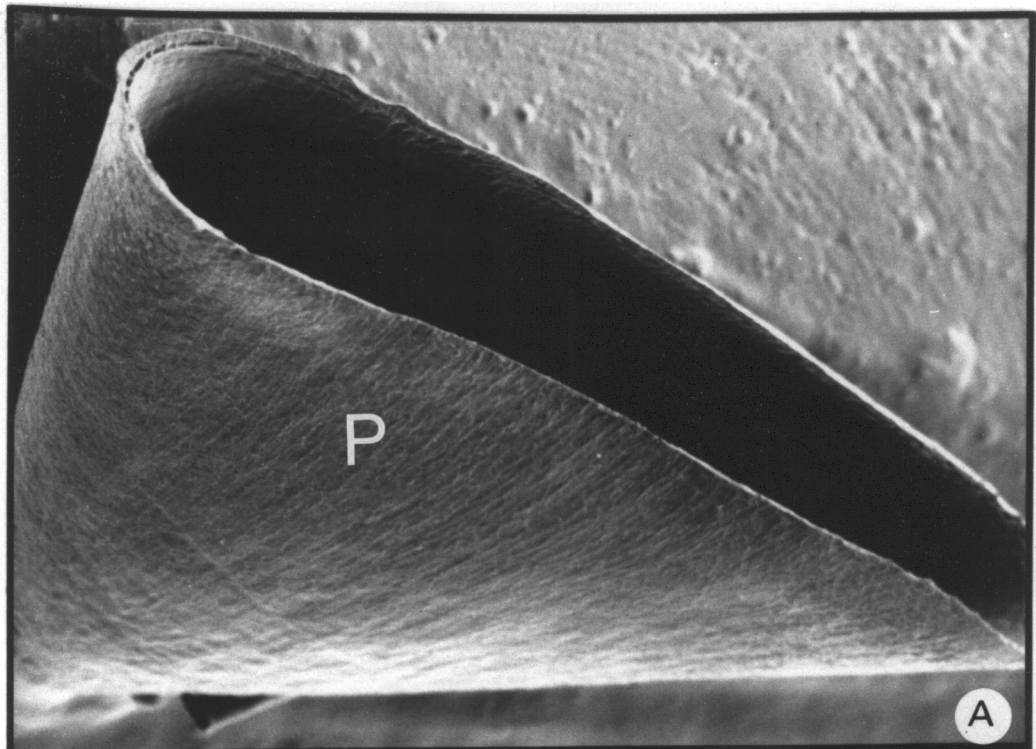


Fig. 2.1. Germination time-course of muskmelon seeds at 25°C. Germination was defined as radicle emergence through the perisperm envelope tissue.

Fig. 2.2 Processed micropylar muskmelon perisperm envelope tissues at 10 h. A) The smooth outer layers are perisperm (P). B) The inner layer is endosperm (E). The outer perisperm tissue is covered with tissues from the testae.



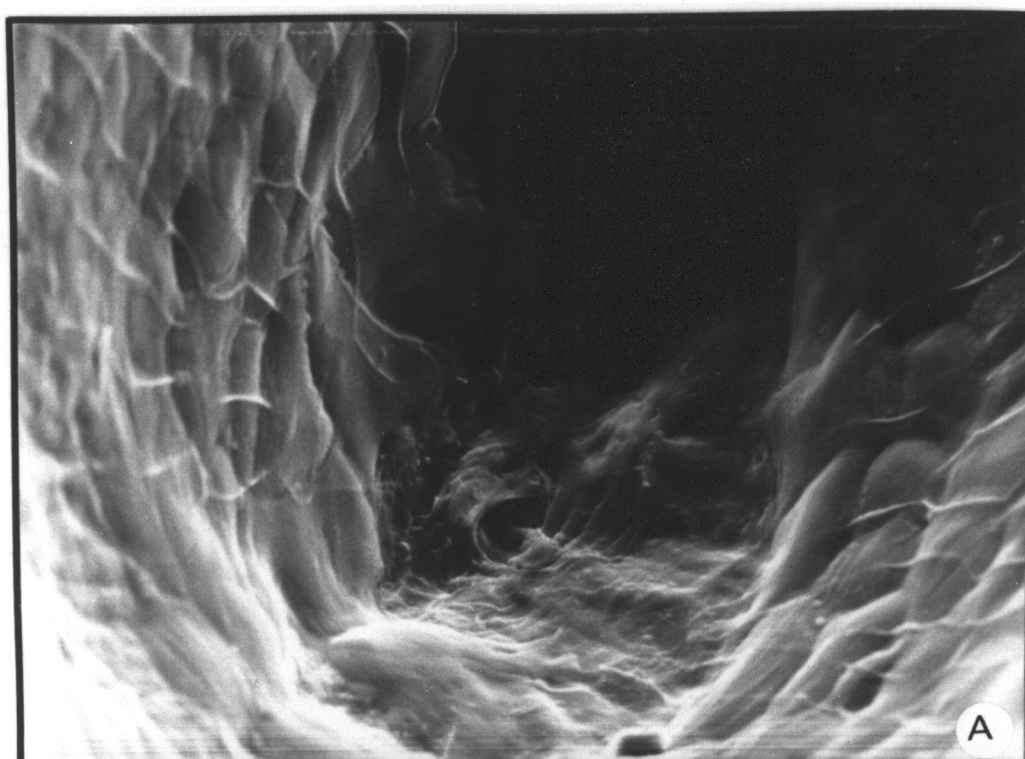
The smooth appearance of the inner surface of the perisperm envelope remained unchanged in all treatments except at the micropylar end (Fig 2.2).

At 10 h, some force was required to separate the adhering embryo from the perisperm envelope. The absence of distinct cellular structure at the tip of some cones may have resulted from damage during extraction (Fig. 2.3). This visible structure was probably the perisperm and not endosperm tissue. Nevertheless, there was no apparent degradation of the perisperm tissue at the micropylar end at 10 h, except for the micropyle at the radicle tip. In tomato and pepper, endosperm degradation was only apparent 1 d prior to radicle emergence (Watkins *et al.* 1985, Groot and Karssen 1987).

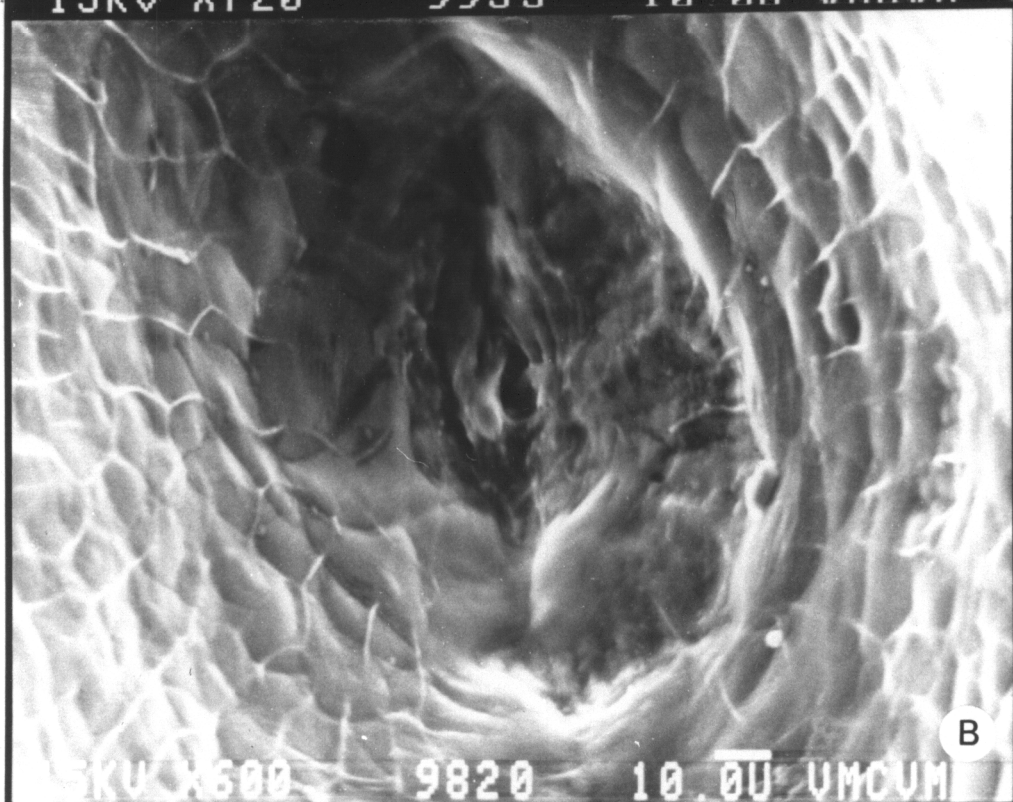
At 15 h, excision of the perisperm cone tips was less difficult. Although some cone tips were damaged during processing, endosperm cells were visible in some undamaged samples. A single layer of endosperm cells, extending from the sides, formed a net-like pattern that stretched across the cone tip (Fig. 2.4). The rectangular endosperm cells had thick cell walls, but the cellular contents were not evident. The smooth perisperm layer was barely discernible beneath the layer of endosperm cells. The appearance of the perisperm tissue at 15 h was very similar to 10 h (Fig. 2.5).

Structural changes were evident in the perisperm envelope at 20 h. Fractures had developed between adjacent cells in some cases, while others were still intact (Fig. 2.6). Degraded endosperm cells directly opposite the radicle tip lacked cellular integrity and appeared crushed, while others were still intact.

Fig. 2.3. Micropylar muskmelon perisperm envelope tissues adjacent to the radicle. There is no apparent degradation of the endosperm tissue at 10 h. A) Processed. B) Fresh-coated.

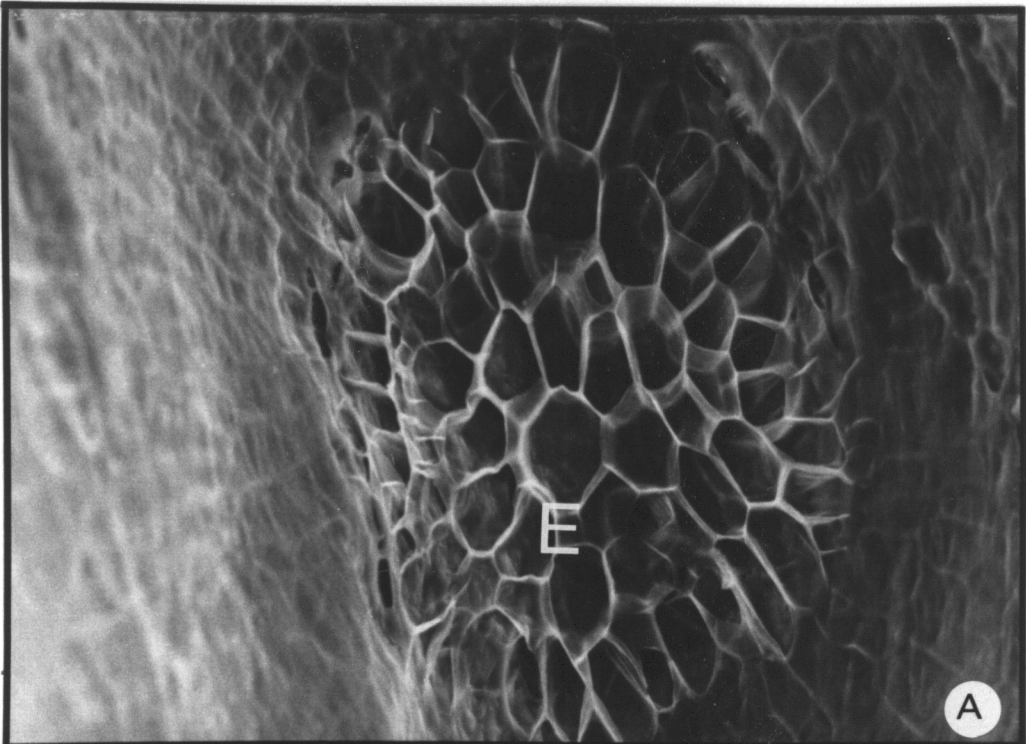


15KV X720 9933 10.00 UMCUM



15KV X600 9820 10.00 UMCUM

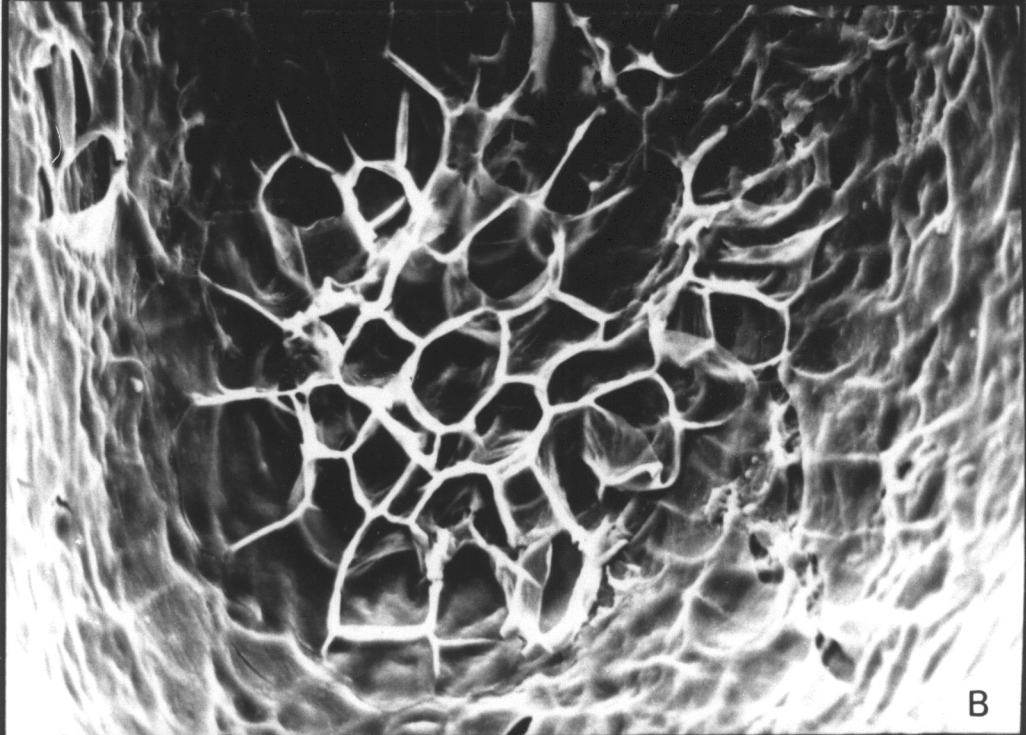
Fig 2.4. Micropylar muskmelon perisperm envelope tissues adjacent to the radicle at 15 h. The endosperm (E) tissue adjacent to the radicle tip is visible. A) Processed. B) Fresh-coated.



15KV X440

9882

10.00 UMCUM

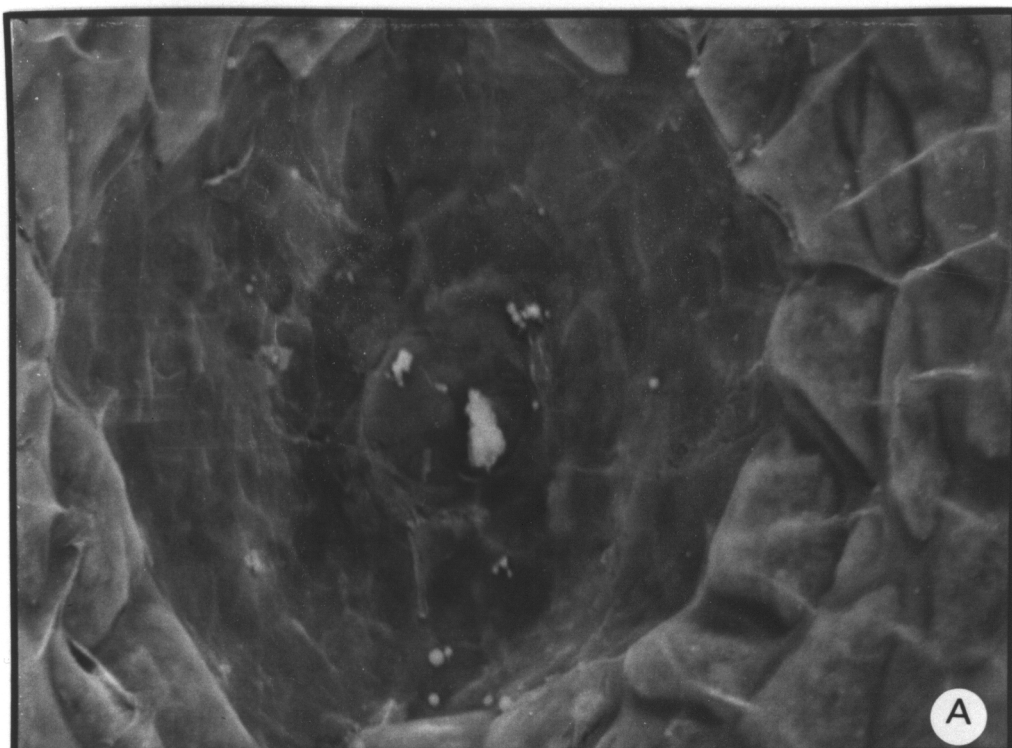


15KV X600

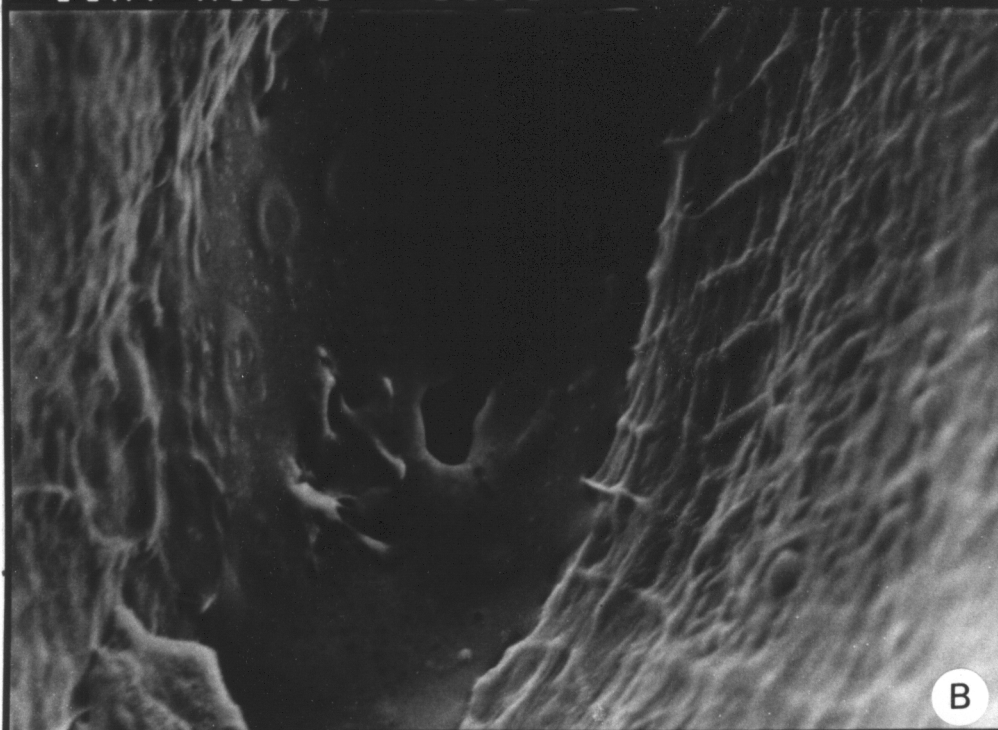
0026

10.00 UMCUM

Fig. 2.5. Micropylar muskmelon perisperm envelope tissues adjacent to the radicle at 15 h. There is no apparent degradation. A) Processed. B) Fresh-coated.

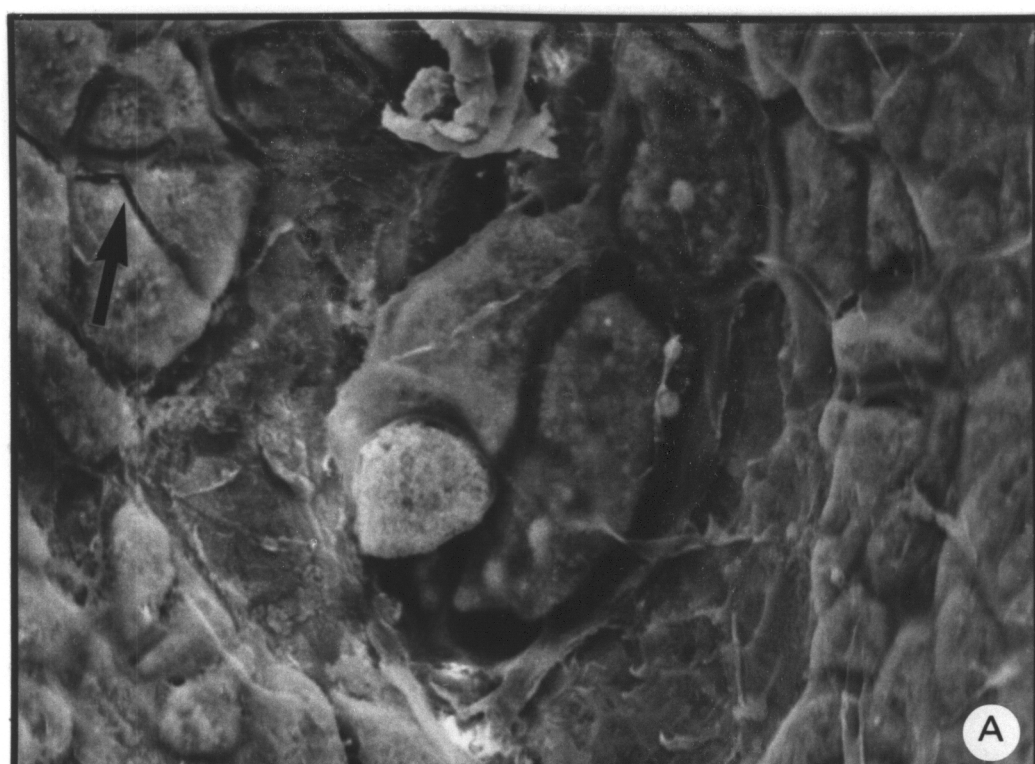


15KV X1000 0008 10.0U VMCUM



15KV X720 9879 10.0U VMCUM

Fig. 2.6. Micropylar muskmelon perisperm envelope tissues adjacent to the radicle at 20 h. Arrow shows a crack between adjacent cells. A) Processed. B) Fresh-coated.



15KV X1000 0034 10.00 UMCUM



15KV X1500 0004 10.00 UMCUM

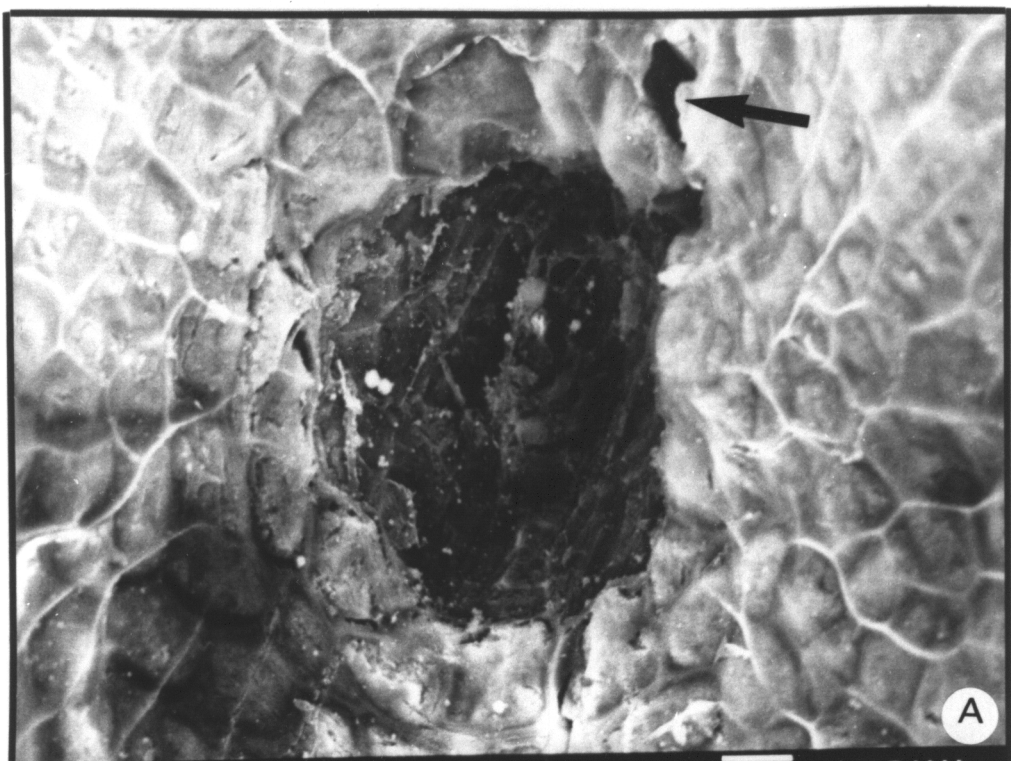
Endosperm degradation in lettuce, tomato, and pepper was exclusively at the radicle tip (Psaras *et al.* 1981, Watkins *et al.* 1987, Haigh *et al.* 1990).

Extensive degradation was evident in perisperm cone tips at 25 h, mostly in the area surrounding the radicle tip (Fig. 2.7). The endosperm cells were severely eroded with obvious loss of cellular contents and wall material. Erosion and fracturing of cells was not uniform in all seeds. By 25 h, a fraction of the seeds had already germinated which may explain the variability in the appearance of the perisperm tissue. Sanchez and coworkers (1990) found a proportion of induced *Datura* seeds with minimal structural alterations of the endosperm at radicle emergence. In germinated muskmelon seeds, the cells at the tip region of perisperm envelope were massively degraded as indicated by severe fracturing and cracking along the sides of the cone tips. In more advanced cases, the remnants of the tip region were fragile and fractured. The lateral cells were still intact with no obvious signs of structural degradation or damage.

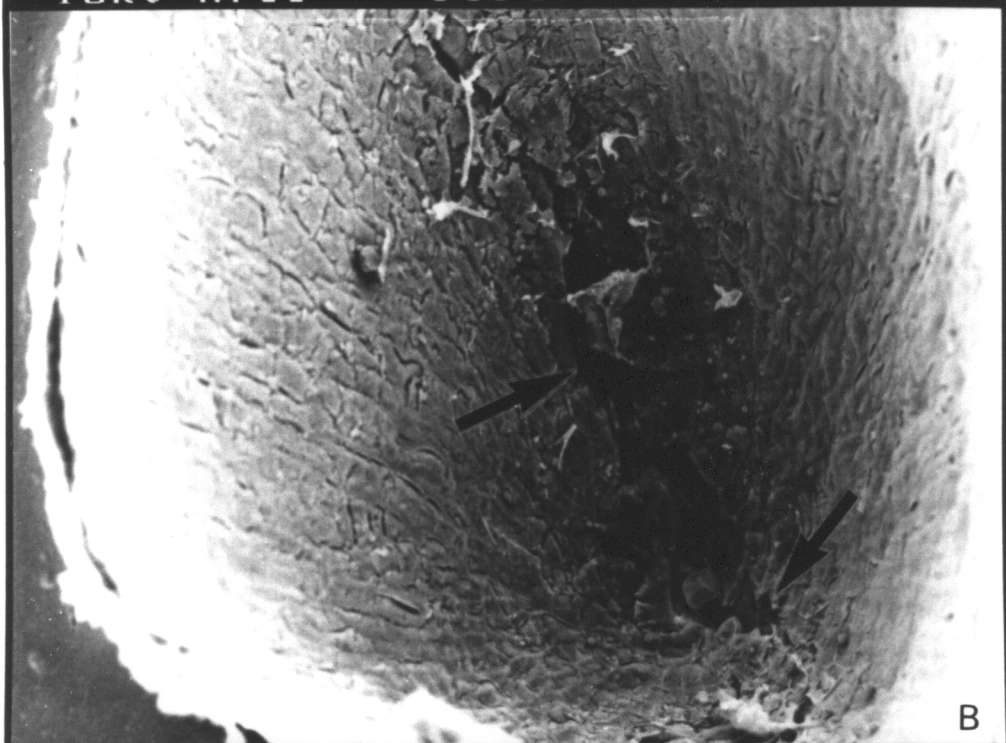
At 30 and 48 h, radicle emergence had occurred as indicated by ruptures and large breaks in the perisperm envelopes (Fig 2.8 and 2.11). In all cases, the cells not in contact with the radicle, were still intact with no signs of degradation.

The outer surfaces of dry, decoated, non-germinated seeds and germinated muskmelon seeds were rough in appearance, because the inner layers of the testa adhere to the outside of the perisperm when the testa is removed (Fig. 2.9, 2.10, and 2.11). In germinated seeds, the perisperm tissue was fractured at the micropylar end to allow radicle protrusion. The fractures enlarged as radicle growth progressed.

Fig. 2.7. Micropylar muskmelon perisperm envelope tissues adjacent to the radicle at 25 h. A) The cracks are more severe. B) Part of the wall is broken. Arrows show cracks.

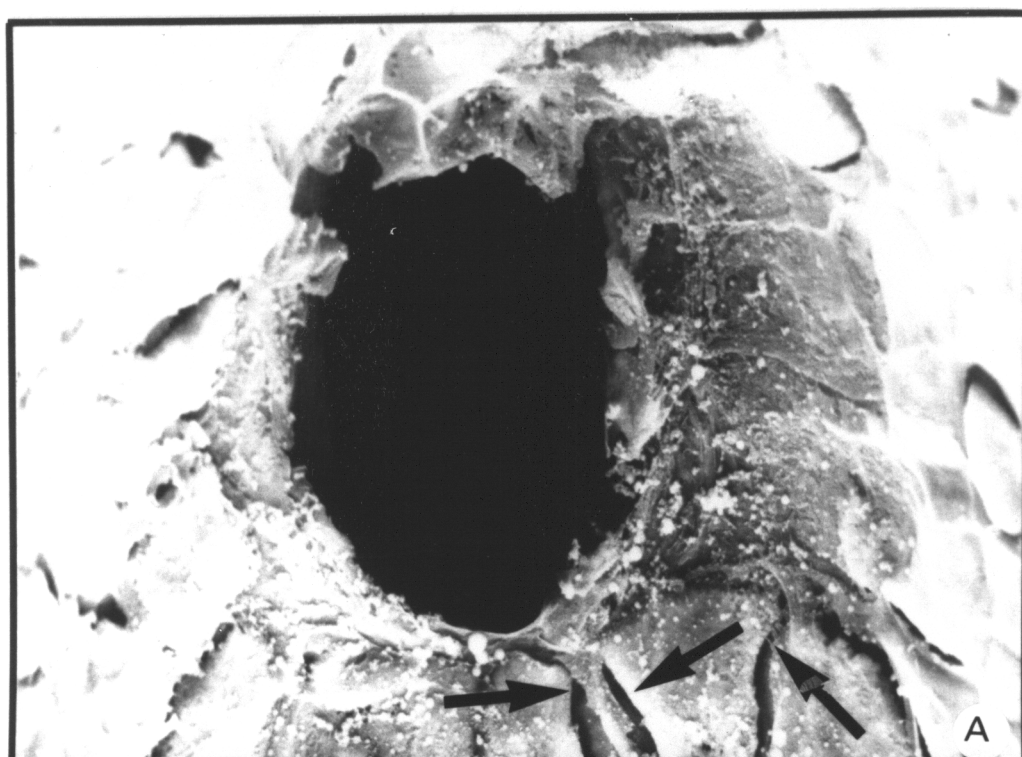


15KV X780 9890 10.0U VMCUM



15KV X200 9950 100.0U VMCUM

Fig. 2.8. Micropylar muskmelon perisperm envelope tissues adjacent to the radicle at 30 h. A) Radicle emergence has occurred as indicated by the large opening. B) The tissue is ruptured by the emerging radicle. Arrows show cracks.



15KV X1000 9975 10.00 VMCUM



15KV X1500 0037 10.00 VMCUM

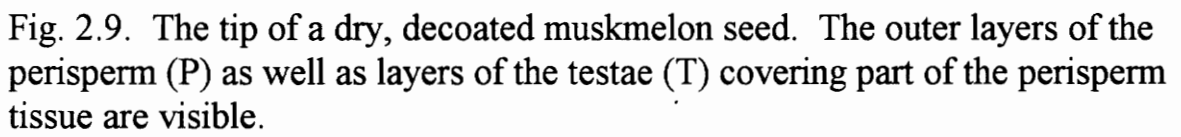
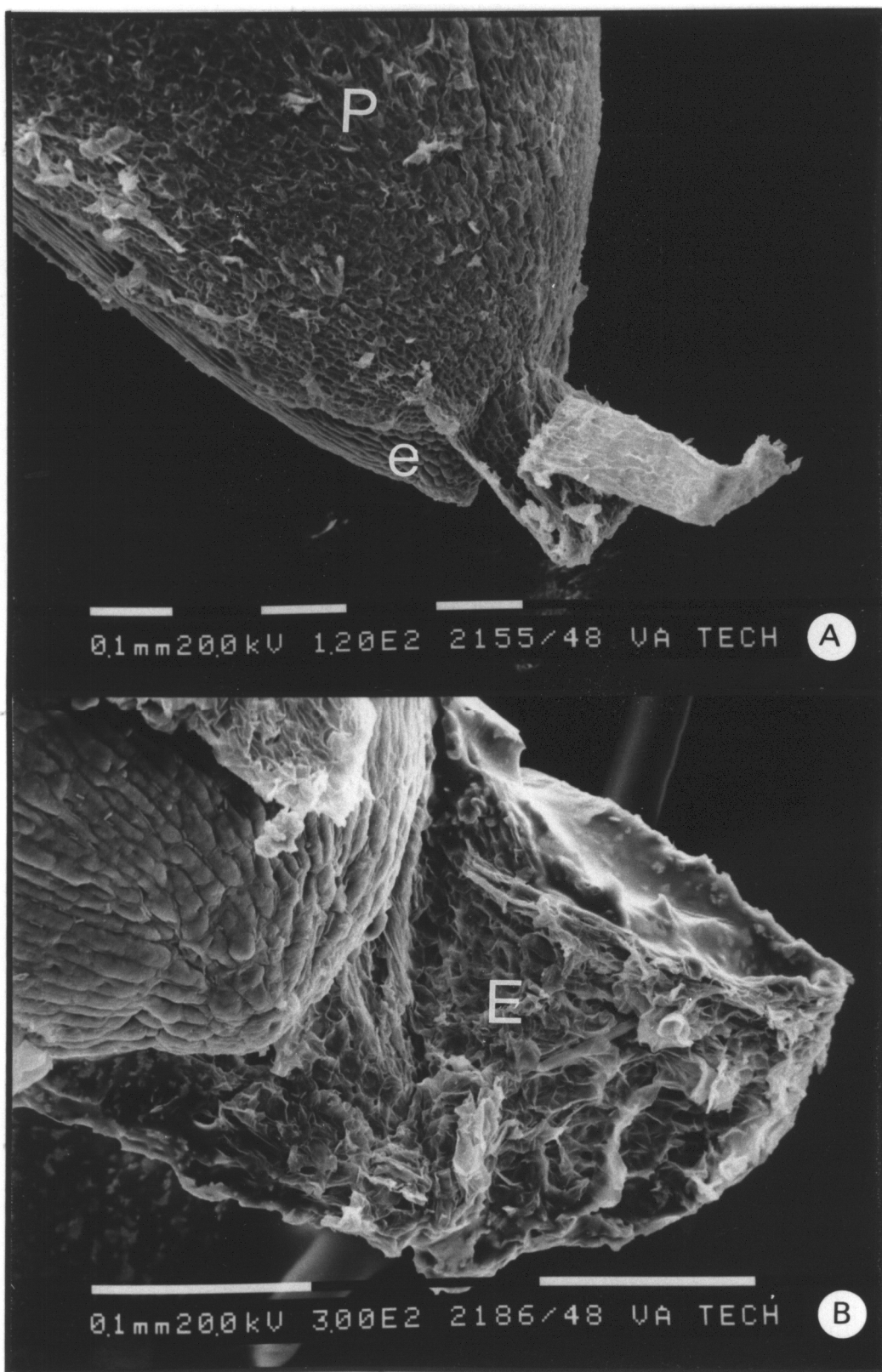
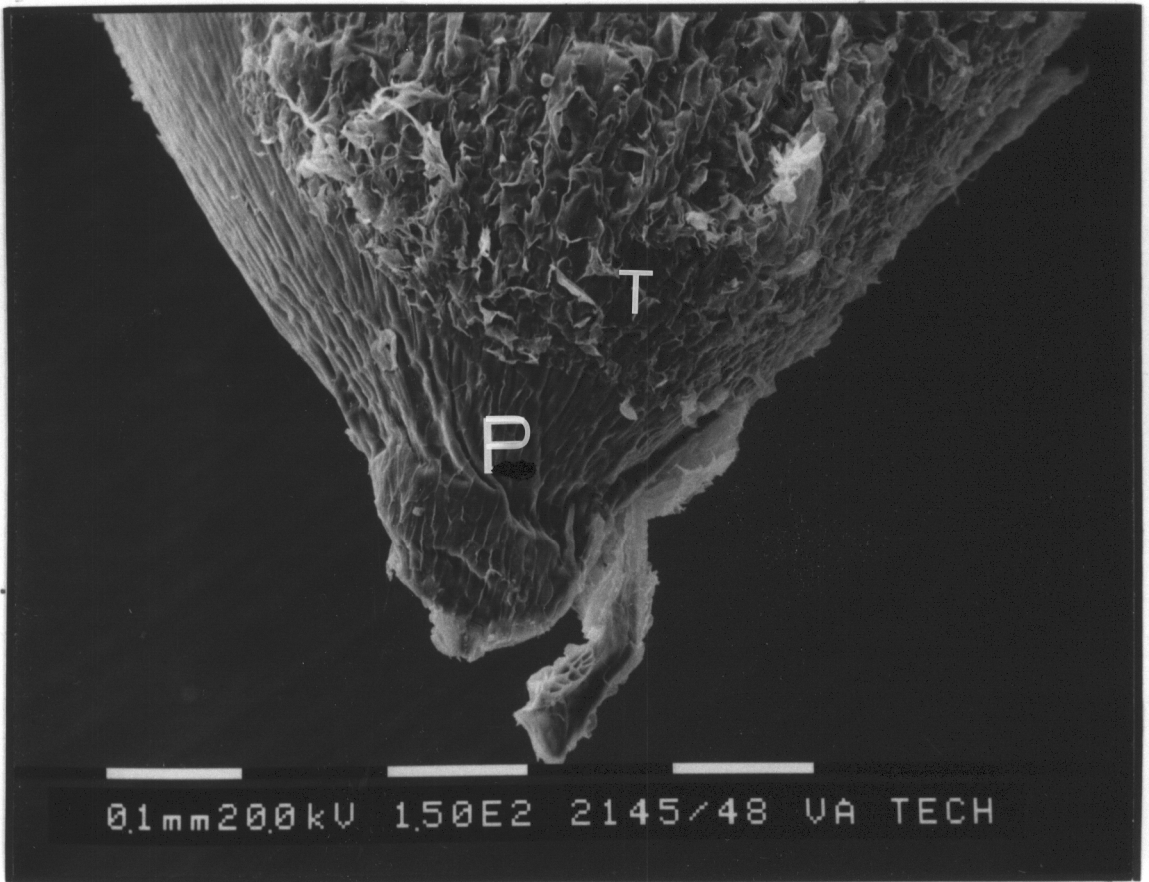
The image is a micrograph showing the tip of a dry, decoated muskmelon seed. It displays the outer layers of the perisperm (P) and layers of the testae (T) covering part of the perisperm tissue. The perisperm appears as a lighter, more granular area, while the testae layers are darker and more structured.

Fig. 2.9. The tip of a dry, decoated muskmelon seed. The outer layers of the perisperm (P) as well as layers of the testae (T) covering part of the perisperm tissue are visible.

Fig. 2.10. The tip of a decoated germinating muskmelon seed at 30 h. A). The perisperm tissue is fractured along sides to allow embryo (e) expansion. B) The degraded endosperm (E) is visible.






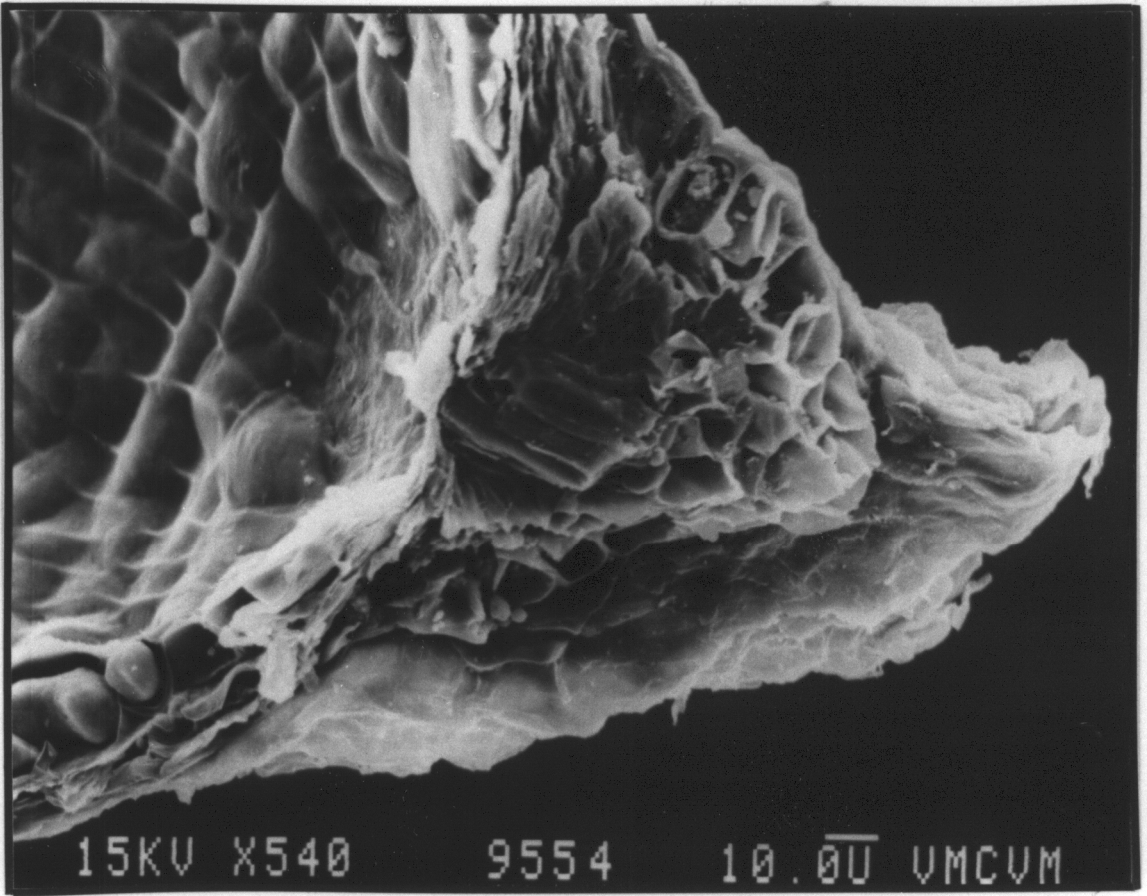


Fig. 2.11. Micropylar muskmelon perisperm envelope tissue adjacent to the radicle at 48 h. The endosperm tissue is degraded and cell contents seem to be missing.



15KV X540

9554

10.0U VMCUM

The ruptured perisperm revealed extensive cell degradation when viewed in cross section. In some cases, the inner surface of the muskmelon perisperm tissue was visible and certainly, structural changes were evident when compared with 10 h seeds.

The results presented clearly illustrate the progressive nature of muskmelon perisperm envelope degradation at the radicle tip during germination. These results are in agreement with those obtained by Pavlista and Valdovinos (1978), Georghiou *et al.* (1983), Psaras *et al.* (1983), Watkins *et al.* (1985), Haigh *et al.* (1990), and Sanchez *et al.* (1990). The lateral cells in muskmelon cone tips, like those of lettuce, tomato, and pepper remained intact throughout the process of imbibition (Psaras *et al.* 1981, Watkins *et al.* 1987, Haigh *et al.* 1990). *Datura* seems to be an exception, because degradation was observed in all three regions of the endosperm (Sanchez *et al.* 1990). Psaras (1984) suggested that micropylar endosperm cells in lettuce were degraded, while lateral cells remained intact during germination, because micropylar cells had a unique role different from the reserve function of lateral cells. The endosperm of lettuce achenes has been considered as a source of food for the growing embryo (Halmer and Bewley 1979). Psaras *et al.* (1981) suggested that actual mobilization of the lettuce endosperm cell wall material did not occur before endosperm rupture. Massive cell wall degradation of the lettuce endosperm was evident after radicle emergence. Endosperm storage material in lettuce is utilized completely after germination (Park and Chen 1974). Similar events probably occurred in muskmelon perisperm cone, tips which might explain the results obtained in this study.

The absence of cellular contents in the perisperm cone tips during germination, may have resulted from enzymatic degradation, or pressure from the expanding radicle, or a combination of both. It is possible that radicle growth resulted from increased turgor in combination with perisperm weakening. In a previous report, turgor of muskmelon embryonic axis remained constant throughout imbibition (Welbaum and Bradford 1990b). These results suggest that degradation of the perisperm envelope is a prerequisite for radicle emergence in muskmelon seeds.

CHAPTER 3

CHANGES IN CELL WALL SUGARS OF MUSKMELON PERISPERM TISSUE DURING IMBIBITION

INTRODUCTION

Among seeds that do not have hard seeds coats, external tissue layers, commonly endosperm or perisperm envelope (perisperm + endosperm), may mechanically restrain embryo expansion (Georghiou *et al.* 1983, Watkins and Cantliffe 1983, Dahal and Bradford 1990, Welbaum and Bradford 1990a). Embryo turgor must exceed the restraining force of the surrounding tissues to allow radicle emergence (Nabors and Lang 1971, Weges 1987, Groot and Karssen 1987, Liptay and Schopfer 1987, Bradford 1990, Sanchez *et al.* 1990). Two mechanisms for overcoming the postulated mechanical restraint have been suggested. The mechanical force of the growing embryo pushing against the surrounding tissues may overcome the resistance, or the combined action of chemical weakening of the barrier tissues and the mechanical force of embryo turgor may also be responsible (Groot and Karssen 1987, Haigh and Barlow 1987, Bradford 1990, Dahal and Bradford 1990, Welbaum and Bradford 1990a).

The cell wall of the lettuce endosperm consists of 60% mannose (Halmer *et al.* 1975). The linear β -(1 \rightarrow 4) mannose residues in lettuce endosperm are presumably linked with β -(1 \rightarrow 4) glucomannans and perhaps

with galactose side-chain substitution (Black and Chapman 1990). The cell-wall mannan is possibly a component of the microfibrillar element present in the thick lettuce endosperm walls (Jones 1974). Biochemical changes in the endosperm of lettuce achenes, stimulated to germinate by red-light or gibberellin application, occur mostly after radicle protrusion (Halmer *et al.* 1976, Bewley and Halmer 1980, 1981, Carpita and Nabors 1981, Leung and Bewley 1981). Endo-(1→4)-β-mannanase is produced in endosperm of lettuce achenes, wherein it acts to break the mannose-based carbohydrates of the cell wall early after radicle emergence (Halmer *et al.* 1975, Dulson *et al.* 1988). Halmer *et al.* (1976) found that mannanase activity in lettuce endosperm was responsible for storage reserve mobilization, but the relationship between mannanase activity and endosperm weakening was not investigated. Alpha-galactosidase is the only enzyme that is clearly enhanced before radicle emergence in lettuce seeds (Leung and Bewley 1981). An increase in carboxymethyl-cellulase has been reported in lettuce prior to radicle protrusion (Pavlista and Valdovinos 1975).

The composition of the endosperm cell wall in two *Datura* species is the same. The endosperm cell walls mainly consist of 4-linked mannan. The timing of mannan loss from the endosperm wall in *Datura* occurs following induction to germinate but prior to radicle emergence. Beta-mannanase production in *Datura* is a phytochrome-controlled process and is responsible for hydrolysis of glucomannans in the endosperm cell wall, thus weakening the endosperm prior to radicle protrusion (Sanchez *et al.* 1990). In seeds of *Datura ferox*, cellulase activity is stimulated by red-light and preceded the earliest signs of endosperm softening (Sanchez *et al.* 1986).

The weakening of tomato endosperm prior to radicle protrusion is mediated by a GA-induced enzymatic degradation of mannan-rich cell walls. The endosperm cell walls in tomato are mannans or galacto-mannans like those of lettuce, fenugreek, and many other species (Groot *et al.* 1988). The GA treatment of isolated tomato endosperm resulted in the appearance of endo- β -mannanase and other hydrolases that were correlated with release of mannose and endosperm weakening (Groot *et al.* 1988). There was no cellulase activity detected in these seeds. Treatment of GA-deficient tomato mutants with GA induced the production of endo- β -mannanase activity that hydrolyzed the mannan-rich endosperm cell walls.

In fenugreek seeds, 30% of the reserve material is galactomannan localized in the endosperm cell wall. The galactomannan in these seeds serves to regulate water-balance during germination and is a substrate reserve for the developing seedling following germination. Endo- β -mannanase, exo- β -mannanase, and α -galactosidase are the major hydrolytic enzymes that depolymerize the galactomannans during fenugreek seed germination (Meier and Reid 1982). The first two enzymes are synthesized *de novo* (Reid and Meier 1972, Reid *et al.* 1977, McCleary 1983) whereas α -galactosidase is in an active state in the resting endosperm (McCleary 1983). The breakdown products galactose and mannose released in the endosperm are absorbed by the embryo. The embryonic axis regulates α -galactosidase activity in galactomannan breakdown (Spyropoulos and Reid 1985).

The pre-germinative decrease in the strength of pepper endosperm was accompanied by an increase in enzymatic activity capable of releasing reducing sugars from wall preparations and galactomannan solutions

(Watkins and Cantliffe 1985). The composition of the pepper endosperm and the specific location of enzyme activity were not determined. Cellulase activity was not detected in these seeds. Considering that tomato, pepper, and *Datura* are all solanaceous plants, it is possible the pepper endosperm wall contains a considerable amount of mannose.

The endosperm of seeds of *Gleditsia triacanthos* consists of a parenchymatic tissue material of branched cells with thick primary walls. The cell walls are built on a network of galactomannans, with high mannose to galactose ratios, reinforced with minor amounts of cellulose (Manzi *et al.* 1990).

The focus of the current research was to identify changes in cell wall composition of the muskmelon perisperm envelope during imbibition using gas and high performance thin-layer chromatography to analyze changes in cell wall sugars. Since changes in cellulose do not seem to be involved in other species, the focus was primarily on changes in the cell wall polysaccharides which appear to undergo the most significant pre-germinative changes in other species. Most of the work on the relationship between endosperm breakdown and radicle emergence has focused on solanaceous crops, little is known about the endosperm cell wall composition in muskmelon.

Chromatography

Chromatography is the separation of chemical substances by partitioning them between two media. One medium or phase is stationary and the other is moving; the first may be solid or liquid, and the second may be liquid or gas. The substances to be separated are distributed between the stationary and the moving phase. Substances are separated from one another based on their solubility in the moving phase and the surface area of the stationary phase. Chromatography provides a means for separating compounds that are very similar, hence difficult or impossible to analyze by other methods (John and Bernard 1987).

Gas-liquid chromatography is a kind of partition chromatography, whereby the stationary phase is a high-boiling liquid, and the mobile phase is an inert gas. For the separation of volatile samples, an inert carrier gas, usually helium or nitrogen, sweeps through a long narrow tube packed with a liquid phase. The sample is introduced at one end of the column and is carried by the inert gas. The column is usually placed in an oven and the separation carried out at one preferred temperature (isothermal) or at variable temperatures. The wall-coated open tubular columns used in this study, are made of glass and have a stationary liquid phase deposited directly on the glass surface. Such columns are capable of high resolution of very small samples. The sample molecules leave the column and pass through a detector. The flame ionization detector (FID) consists of a hydrogen-air flame burning at the end of a capillary tube. When organic substances are introduced into the flame, ions are formed and collected by applying a voltage

across the flame. The current resulting from the ion collection is amplified and recorded. The FID has a relatively high sensitivity for detection of organic compounds but does not respond to water, carbon monoxide, carbon dioxide, or inert gases and produces a stable base line minimally affected by changes in temperature. The detector response is recorded, and both the position (time) and the size of the response are used to quantify and identify substances being separated. The retention time (position of the peak) is used for identification by comparison with the retention time of known standards. The area under the peak is used to estimate the amount of substance present (John and Bernard 1987).

Thin-layer chromatography involves finely powdered adsorbents such as silica gel. The powdered solid absorbent, usually mixed with a binder (*e.g.*, 10% calcium sulfate), is spread as a thin (0.2 to 0.5 mm), uniform coat over the surface of a glass plate or a plastic sheet. The purpose of the absorbent is to increase resolving power as well as the speed of separation. The fine particle size (0.1 mm) provides a high surface-to-volume ratio, giving a large active surface area for a given amount of absorbent. Furthermore, the high surface area of the absorbent also increases the flow rate of the solvent.

Corrosive detecting reagents such as sulfuric acid can be sprayed onto the plates, giving sensitive and simplified detecting systems, due to the relatively inert nature of the inorganic adsorbents. The high level of sensitivity is achieved by concentrating the material into small spots through several chromatogram developments. The spray reagents react with the standard carbohydrates, and the resultant color stands out clearly against an

almost white background (Adachi 1965). The minimum amount of material that can be detected on a thin-layer chromatogram is 0.1 to 0.05 μ moles.

Recent improvements in high performance thin-layer chromatography (HPTLC) systems allow accurate quantitative determinations of sugars utilizing densitometric scanners after chromatogram development and visualization. Thin-layer chromatography offers several advantages over other techniques, including ease of sample preparation and simultaneous analysis of multiple sugars. In addition, HPTLC provides a high degree of analytical precision and decreases the time required for analysis (Lee *et al.* 1979).

MATERIALS AND METHODS

Plant material

Muskmelon (cv. Top Mark) seeds were harvested 50 d after anthesis in 1987. The seeds were stored at 5°C at a moisture content of 6% (dry weight basis) until the start of the experiment.

Time-course for germination

Fifty seeds were incubated at 25°C in 9 cm petri dishes on two thickness of germination blotter paper (Anchor Paper Co.) moistened with 10 ml of distilled water. After the first 12 h, seeds were observed every 2 h for radicle emergence.

Incubation conditions

Fifty seeds were incubated at 25°C for 10, 15, 20, and 25 h. At the end of each incubation period, seeds were frozen in liquid nitrogen to arrest germination uniformly and to facilitate removal of the perisperm envelope. The seeds were decoated and dissected to isolate approximately 0.5 mm micropylar perisperm cone tips from the remainder of the perisperm envelope tissue.

Extraction of cell walls

The perisperm cone tips were collected in ice cold 80% ethanol and processed immediately or stored in a freezer at -30°C for a period not longer than one week. Ethanol was decanted, and the samples ground with a mortar and pestle. Using a glass homogenizer, samples were ground further in 100 mM potassium phosphate (pH 7.0), and the homogenate was centrifuged for 10 min at 1000 g. The pellet was suspended in 2 M sodium chloride, centrifuged, and washed successively with distilled water and methanol. The pellet (cell wall fraction) was resuspended in chloroform:methanol (1:1, v/v) on ice for 15 min and occasionally shaken. After centrifugation, the pellet was washed with methanol and water successively and then freeze dried (Sanchez *et al.* 1990).

Gas chromatography

Sugar standard

The sugar standard mixture consisted of 0.02 mmole of rhamnose, fucose, ribose, arabinose, xylose, mannose, galactose, glucose, galacturonic acid, and glucuronic acid in 1 ml of distilled water.

Trimethylsilyl derivation of cell wall sugars: TMS Ethers of Methyl Glycosides

For each sample to be analyzed, approximately 1 mg of dry cell wall was added to a 13 x 100 mm screw-top tube (exact weight was recorded). To another tube, 25 μ l of the standard sugar mixture was added. To each sample, 100 μ g of internal standard (20 μ l of 5 mg ml⁻¹ myo-inositol in distilled water) was added and blown dry with a stream of air at room temperature. After the addition of 500 μ l of 1 M hydrochloric acid in methanol, samples were heated for 15 hrs at 80°C. The 1 M HCl in methanol was prepared by slowly adding 3.55 ml acetyl chloride into 50 ml methanol in an ice bath. The acid hydrolysis converts the polysaccharide into a mixture of methyl glycosides and methyl ester glycosides of the glycosyluronic acids (York *et al.* 1984). The methanolic HCl was removed by adding 100 μ l of t-butyl alcohol and then evaporated with a stream of filtered air at room temperature. The methyl glycosides and methyl ester glycosides were silylated using 200 μ l pyridine, 40 μ l hexamethyldisilazane, and 20 μ l of trimethylchlorosilane, mixed in these proportions as Tri-sil (Sigma Chemical Company). Samples were heated for 20 min at 80°C and gently evaporated at room temperature until a viscous residue was obtained. The derivatives were redissolved in 1 ml of hexane. Samples were vortexed and centrifuged for 2 min at 6000 g to remove insoluble salts. The supernatant was transferred to clean 13 x 100 screw-top tubes and carefully evaporated at room temperature. The residue was

redissolved in 500 µl hexane, and 1 µl of this solution was analyzed by gas chromatography (Albersheim *et al.* 1974).

Quantitative analysis

Gas chromatographic (5840A, Hewlett Packard) analysis of the trimethylsilyl derivatives was achieved using an Alltech capillary column [30m x 0.25 mm (i.d.)] SE - 30. A 1 µl sample was introduced into the GC using a drop-needle injector. The carrier gas was hydrogen. The temperature program was as follows: 5 min at 140°C, then 2°C/min to 180°C, then 30°C/min to 275°C, followed by a 10 min hold (York *et al.* 1984). Quantification of ionized sugars was achieved by a flame ionization detector. Peak areas were integrated by a 5840A Hewlett Packard Integrator. Sugar concentrations in the samples were calculated using the following formula:

µmole sugar in the sample =

Peak area - sugar (sample)

Peak area - internal std (sample) x 0.5 µmole

Peak area - sugar (standard)

Peak area - internal std (standard)

High Performance Thin-Layer Chromatography

Sugar standard

The sugar standards were the same as those used for gas chromatography. A series of three concentrations of mixed standards were hydrolyzed along with the cell wall samples.

HCl in methanol hydrolysis

For each sample to be analyzed, approximately 1 mg of dry cell wall and 30 ml of each sugar standard were added to a 1 ml disposable microcentrifuge tube (exact weight was recorded). The samples were hydrolyzed using the same method described for gas chromatography. The method allowed for rigorous water exclusion by the methanol molecules that were added across the glycosidic linkage to afford the methyl glycosides (Bierman 1988). The methanolic HCl was removed by adding 100 μ l of t-butyl alcohol and then evaporating with a stream of filtered air at room temperature. The resulting components were resuspended in 50 ml of 70% ethanol.

Trifluoroacetic acid (TFA) hydrolysis

The dry cell wall material (0.5 to 1 mg) were hydrolyzed in 500 μ l of 2 M TFA for 2 h at 121°C. After centrifugation, the TFA-insoluble pellet was

washed with 80% ethanol. Trifluoroacetic acid was removed from the samples in a stream of filtered air, and the TFA soluble material was resuspended in 50 ml of 70% ethanol.

HPTLC plates

Merck pre-coated silica gel plates for HPTLC (10 x 10 cm) were used for all HPTLC. The plates were pre-washed in methanol (Sigma HPTLC grade) and dried with heated air before use. After the pre-wash, the plates were pretreated by spraying with a 0.1 M sodium sulfate solution (Mahran *et al.* 1991) or a 0.1 M sodium bisulfite buffer solution (Fell 1990). Plates were dried and then sprayed with a citrate buffer (1:10 dilution of Sigma citrate buffer with water pH 4.8) to improve sugar separations (Pruden *et al.* 1975, Ghebregzabher *et al.* 1976). The plates were placed in a drying oven at 100°C for 24 h. Following the final heat activation, the plates were transferred to a desiccator for storage. Pretreated plates could be stored up to eight weeks before use (Fell 1990).

Solvents

- A. Ethyl acetate-acetic acid-methanol-water (12:3:3:2)
- B. Propanol-water (85:15)
- C. Propanol-water (88:12)
- D. Propanol-water (90:10)
- E. Propanol-water (95:5)

Sample application and development

Sample solutions were applied using a Camag Nanomat 1 applicator and Camag microcaps. Samples were spotted in 0.1 and 0.5 μl volume for high sensitivity. Smaller sample volumes provided better sensitivity and quantitative measurements in the 30 to 500 ng range. After spotting, the samples were dried for 1 min with heated air before development. Three- to four millilitres of fresh developing reagent were added to the twin trough chambers before each run. The solvent was allowed to run to 7 - 9 cm from the bottom of the plate (6.5 cm to 8.5 cm from the origin), and average elution time per plate varied with the reagent (30 to 180 min). Plates were developed two to three times in the same direction depending on the reagent. The plates were dried thoroughly for 1 min between each run, because incomplete drying may cause diffuse spots, streaking, and a variable solvent front (Fell 1990). After final development and drying, the plates were sprayed or dipped into a tank containing the developing reagent. Plates were heated in a drying oven to char the sugars for visualization (Pruden *et al.* 1975). Gentle brushing of the plates with a camel hair brush, after the final drying and before dipping, helped to remove small particles of lint and dust that char during the visualization heating. This provided a cleaner background and better visualization (Fell 1990).

Visualization

The plates were dipped or sprayed with a thymol-sulfuric acid reagent (Kartnig and Wegschaider 1971, Lenkey and Nanasi 1986). The reagent was prepared by dissolving 0.5 g thymol in 95 ml ethanol (95%). Concentrated sulfuric acid (5 ml) was carefully added to the solution. The reagent was stored in the dark at 4°C and was stable for 2 d. Plates were heated for 5 min at 105°C. Sugars appeared as colored spots on an almost white background unless the plates were overheated. The colors stabilized after 30 to 60 min.

Quantitative analysis

Quantitative measurements were made by absorbance scanning using a CAMAG TLC Scanner II, interfaced to an Sp-4270 integrator. The plates were scanned at a wavelength of 440 nm, using a slit length of 3 mm and slit width of 0.2 mm. Slit length and width were selected to reduce noise-to-signal ratios and to maximize sensitivity (Poole *et al.* 1985). Instrument sensitivity and span settings were 190 and 20, respectively. Integrator parameters were set according to the CAMAG TLC program with a peak width of 1 and peak threshold value of 1000. All scans were made in the direction of chromatographic development, and peak areas were used for quantification. A series of mixed standards of three concentrations was run with each plate. Values obtained from standards were used for the construction of a standard curve for each sugar.

RESULTS AND DISCUSSION

Germination timing among seeds was variable, and by 25 h radicle emergence was evident in some cases. Seeds without radicle emergence were used for the study.

Acid hydrolysis was used to determine the monosaccharide composition of cell walls by GC and HPTLC (Albersheim *et al.* 1967, Biermann 1988, Sanchez *et al.* 1989). Hydrolysis, cleavage of a bond by addition of the elements of a water molecule, is the most common method of cleavage of glycolytic linkages. The conditions for acid hydrolysis were controlled to try to ensure that complete hydrolysis was obtained with little or no degradation of the monosaccharide units. Generally, with any of the methods used for acid hydrolysis, there is always a trade-off between incomplete cleavage of the glycosidic linkage under relatively mild conditions and decomposition of the liberated monosaccharides under more severe conditions (Biermann 1988). Peak identification from GC output was complicated by numerous peaks that possibly occurred from incomplete hydrolysis of the samples (Fig. 3.1).

The results obtained from the GC are based on one sample (representing approximately 50 perisperm envelope cone tips) at each time interval, because the study was discontinued due to mechanical breakdown. Nine sugars were detected from the perisperm cone tips using the GC (Fig. 3.2, and 3.3). The sugars decreased within the first 15 h of imbibition followed by a sharp increase in most of the sugars prior to radicle emergence.

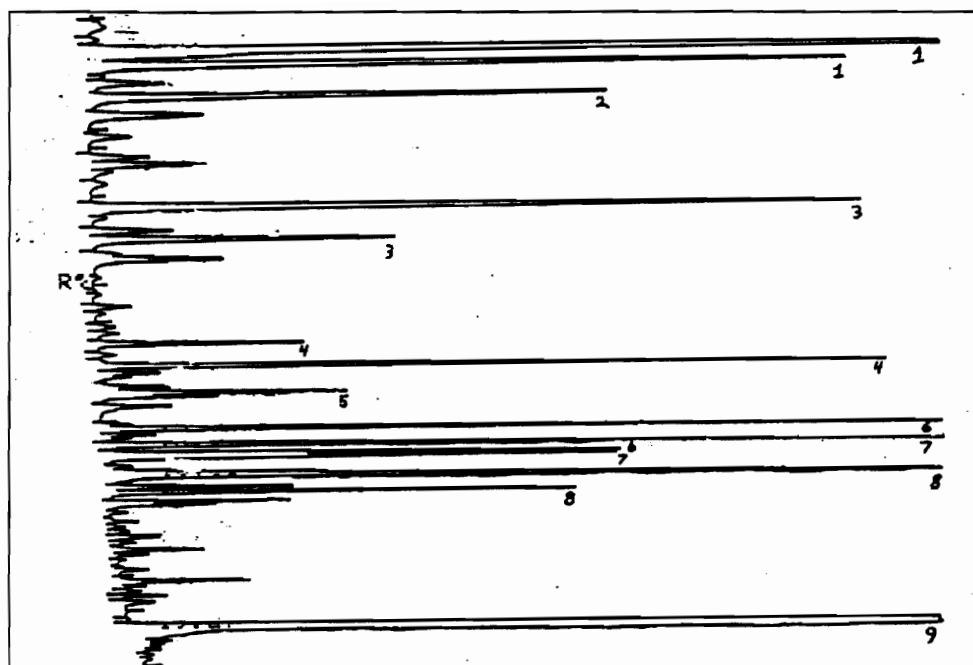


Fig. 3.1. GC recordings of cell wall sugars of muskmelon perisperm cone tips from seeds imbibed for 25 h. Arabinose (1), rhamnose (2), fucose (3), xylose (4), galacturonic acid (5), mannose (6), galactose (7), glucuronic acid (8), glucose (9) and Myo-inositol (internal standard) (10).

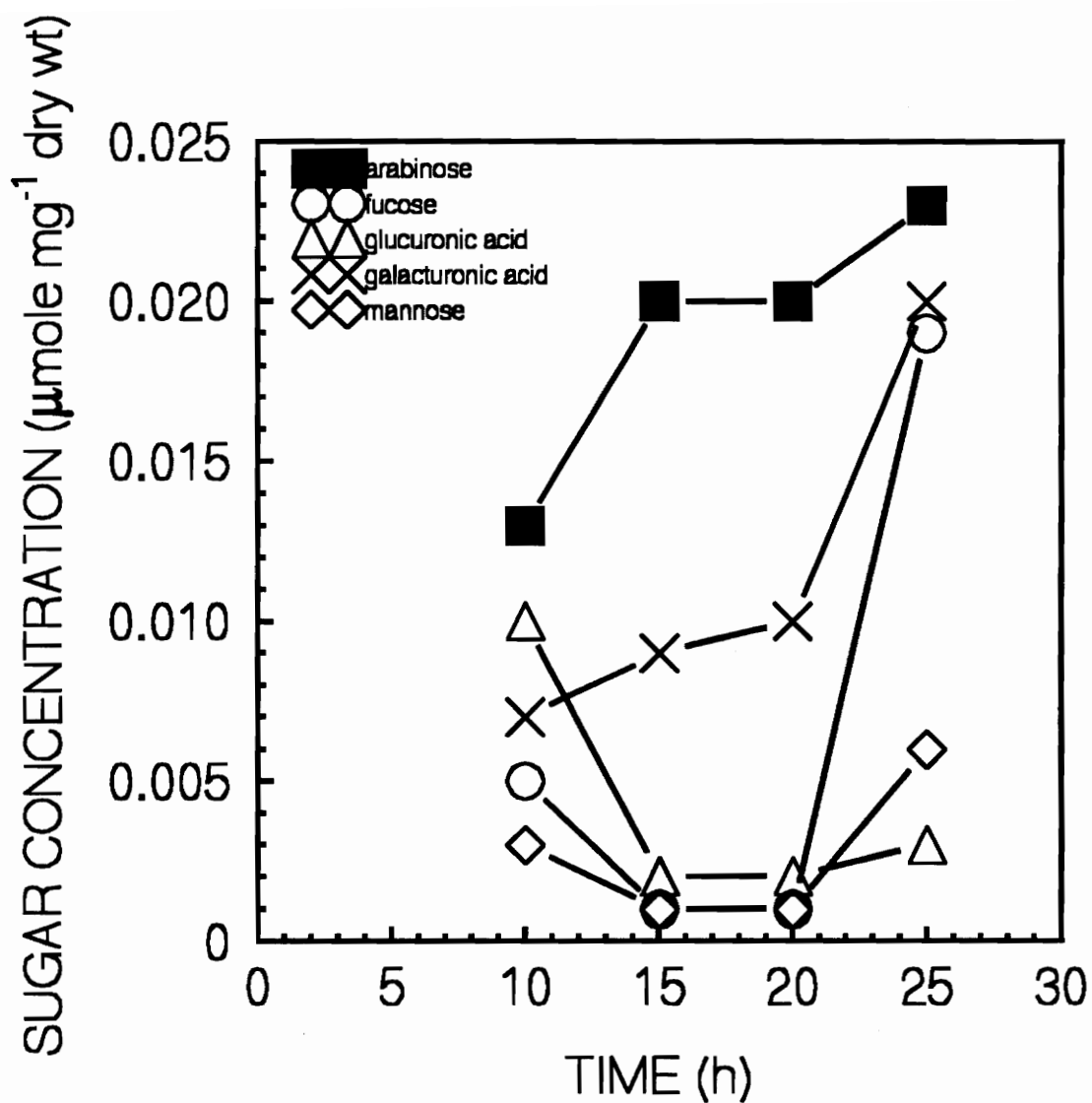


Fig. 3.2. The changes in cell wall sugars of muskmelon perisperm cone tips determined by GC during imbibition.

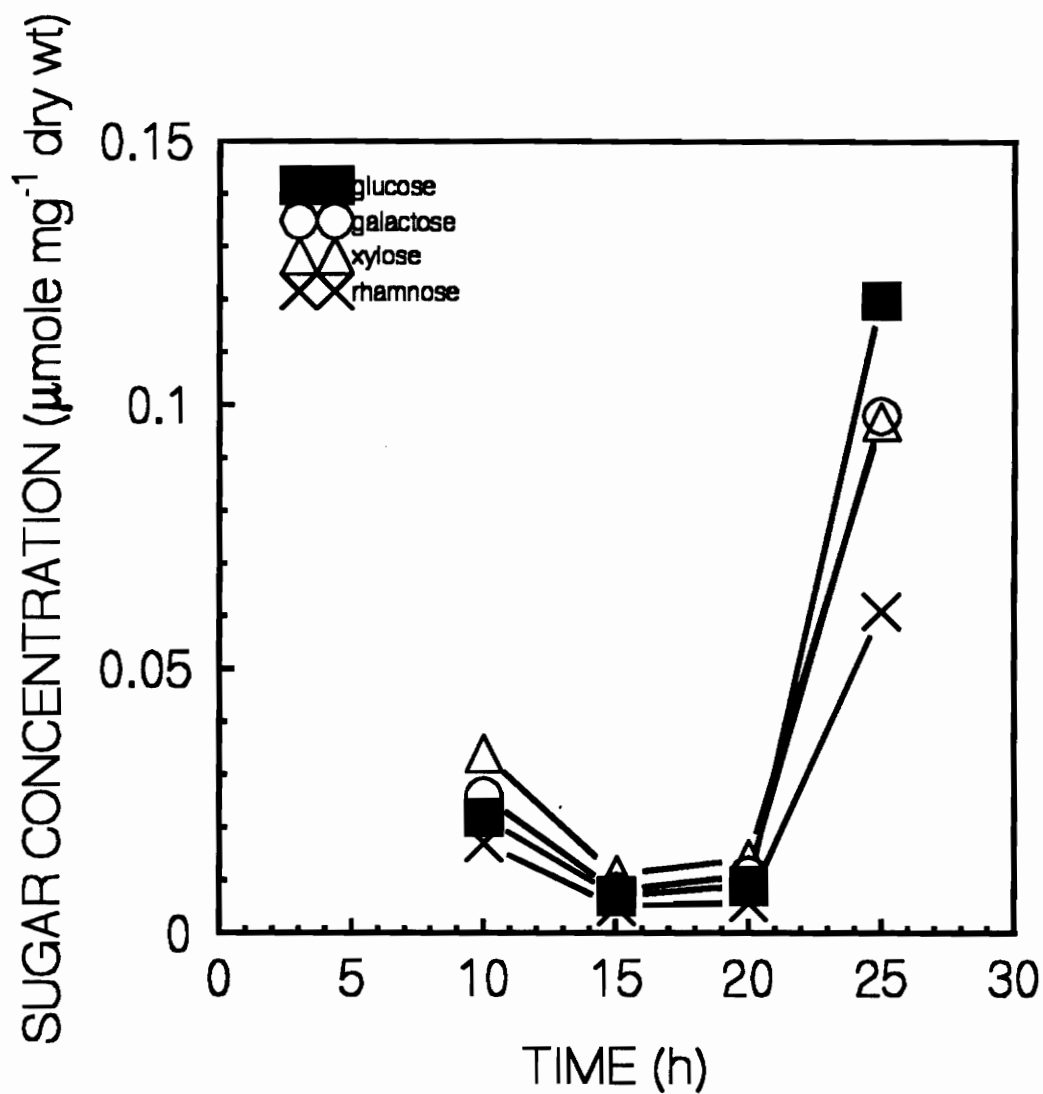


Fig. 3.3. The changes in cell wall sugars of muskmelon perisperm cone tips determine by GC during imbibition.

At 25 h, the muskmelon cone tips contained relatively larger amounts of rhamnose, xylose, glucose, and galactose than arabinose glucuronic acid, galacturonic acid, fucose, and mannose.

Sugar analysis by HPTLC was easier and repeatable compared to GC. The sugars contained in the standards yielded different colors after treatment with the reagent, thus enabling easier identification (Table 3.1). All the solvents were incapable of separating galactose from glucose except solvent D (Fig. 3.4a) and to a lesser extent solvent A (Fig. 3.4b). Solvent A required only 30 min for a single development compared to 120 to 180 min required for solvents B, C, D, and E. Although solvent E gave relatively good separation, solvent migration was faster and resulted in severe streaking of the spots. As a result, solvent D was used to obtain the results shown in Figures 3.5, 3.6, and 3.7.

Calibration curves (Fig. 3.8) were made at the same time and on the same plate as the samples, because the results varied widely from plate to plate depending on the prevailing conditions. Lenkey *et al.* (1986) proved that the density of the same spots is different from chromatogram to chromatogram, and that the density depended on the amount of thymol used, the temperature of the oven, and the time of detection of spots.

As opposed to the GC, only four sugars were detected in the perisperm envelope tissue by HPTLC (Fig. 3.5, 3.6, and 3.7). The change in sugar concentration during imbibition followed a similar pattern to that obtained using GC. The perisperm envelope cone tips contained relatively large amounts of glucose and galactose in the perisperm cone tips and lesser amounts of xylose and rhamnose.

Table 3.1: Sugar standards developed in propanol:water. (90:10).
Visualization: thymol-sulfuric acid reagent

| Sample | R _f | Color |
|-------------------|----------------|-------------------------|
| Rhamnose | 0.90 | orange, violett |
| Xylose | 0.77 | light purple |
| Fucose | 0.69 | Orange with dark center |
| Ribose | 0.55 | dark purple |
| Mannose | 0.50 | pink |
| Galactose | 0.40 | red with dark center |
| Glucose | 0.37 | light-pink |
| Arabinose | 0.32 | light purple |
| Glucuronic acid | 0.08 | beige |
| Galacturonic acid | 0.03 | beige |

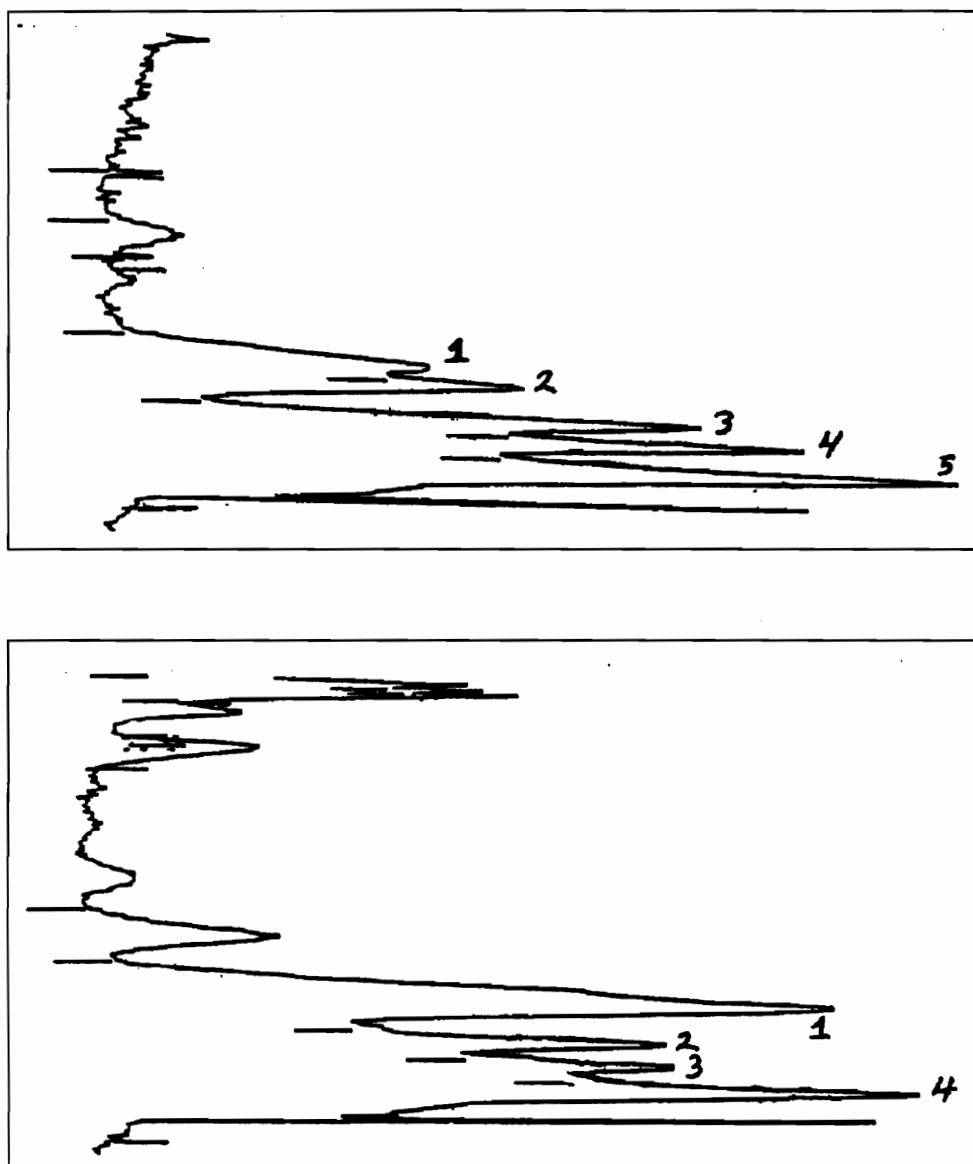


Fig. 3.4. Scanner recordings of cell wall sugar chromatograms of muskmelon perisperm envelope tissue on silica gel 60 HPTLC plates, developed with two different reagents 25 h after the start of imbibition. A) solvent D (propanol:water, 90:10) gave Glucose (1), galactose (2), xylose (3), rhamnose (4), solvent front (5). B) Solvent A (Ethylacetate:acetic acid:methanol:water, 12:3:3:2) gave Glucose and galactose (1), xylose (2), rhamnose (3), solvent front (4).

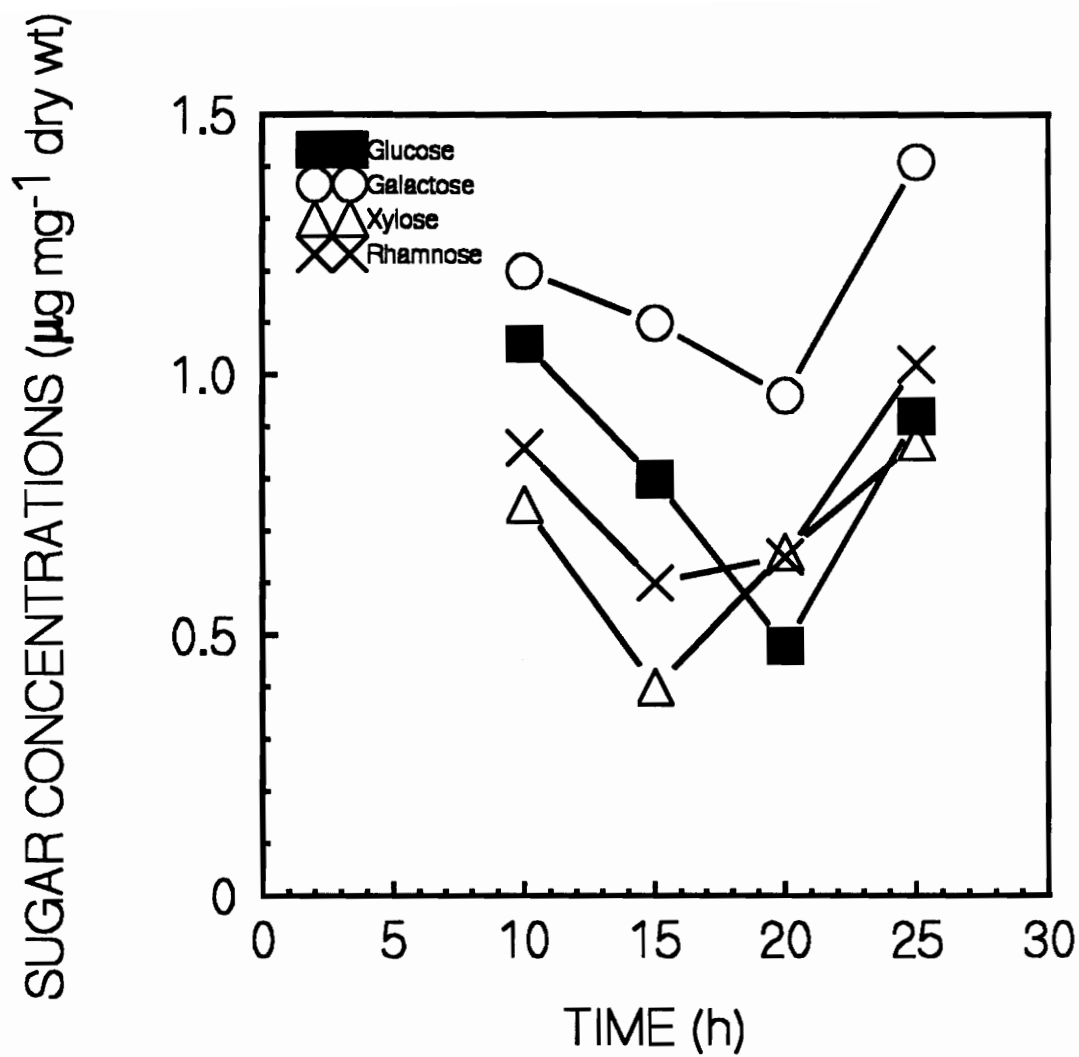


Fig. 3.5 Changes in sugar concentrations determined by HPTLC in the cell walls of muskmelon perisperm cone tips during imbibition.

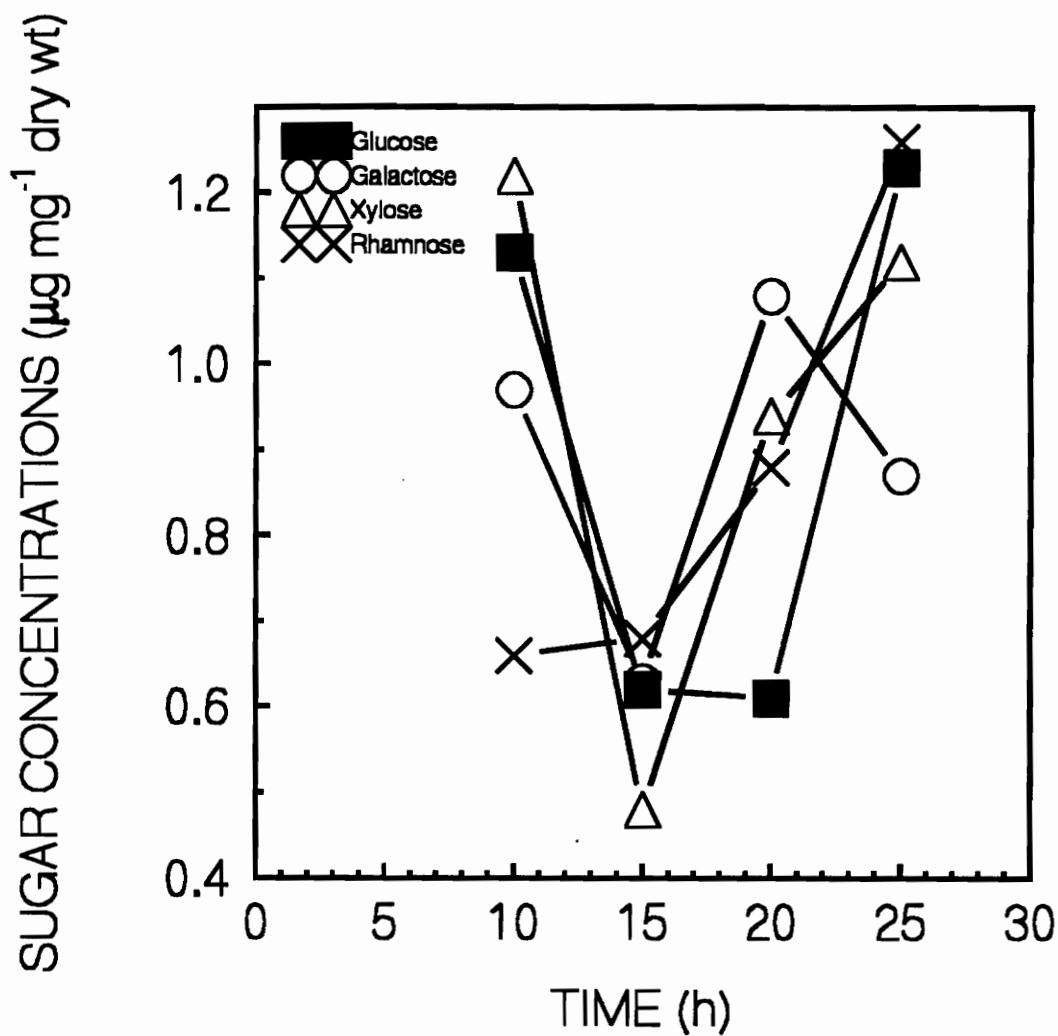


Fig. 3.6. Changes in sugar concentrations determined by HPTLC in the cell walls of muskmelon perisperm tissue without cone tips during imbibition.

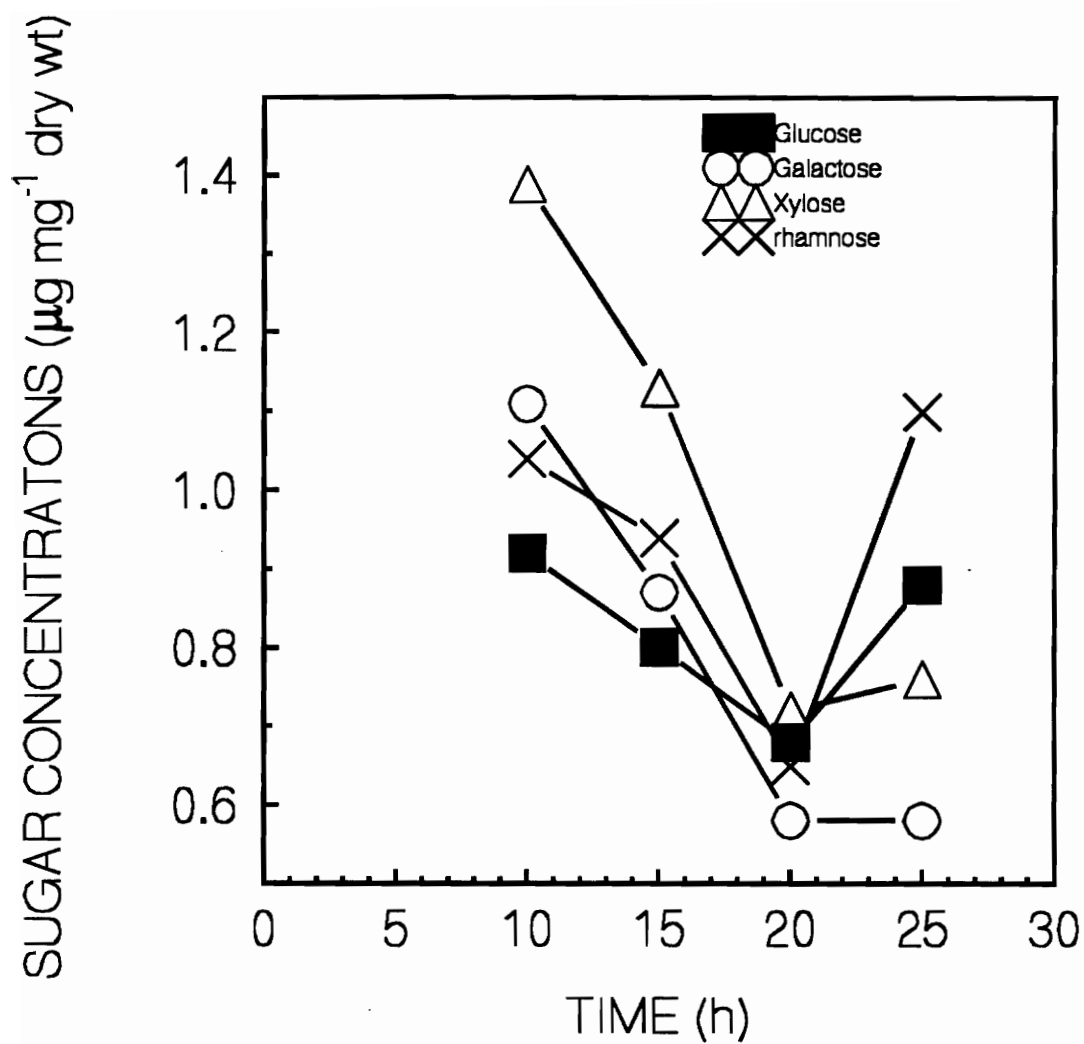


Fig. 3.7. Changes in sugar concentrations determined by HPTLC in the cell walls of intact muskmelon perisperm envelope during imbibition.

Table 3.2. Monosaccharide concentrations ($\mu\text{g mg}^{-1}$ dry weight) in cell walls of muskmelon perisperm tissue cone tips determined by HPTLC.

| Sugar | <u>10 h</u> | <u>$\pm\text{se}$</u> | <u>15 h</u> | <u>$\pm\text{se}$</u> | <u>20h</u> | <u>$\pm\text{se}$</u> | <u>25h</u> | <u>$\pm\text{se}$</u> |
|-----------|-------------|----------------------------------|-------------|----------------------------------|------------|----------------------------------|------------|----------------------------------|
| Glucose | 1.06 | 0.23 | 0.80 | 0.33 | 0.48 | 0.56 | 0.92 | 0.38 |
| Galactose | 1.20 | 0.48 | 1.80 | 0.04 | 0.96 | 0.22 | 1.41 | 0.42 |
| Xylose | 0.75 | 0.26 | 0.40 | 0.16 | 0.66 | 0.19 | 0.85 | 0.09 |
| Rhamnose | 0.86 | 0.34 | 0.60 | 0.07 | 0.65 | 0.15 | 1.02 | 0.15 |

Table 3.3. Monosaccharide concentrations ($\mu\text{g mg}^{-1}$ dry weight) in cell walls of muskmelon perisperm tissue without cone tips determined by HPTLC.

| Sugar | <u>10 h</u> | <u>$\pm\text{se}$</u> | <u>15 h</u> | <u>$\pm\text{se}$</u> | <u>20h</u> | <u>$\pm\text{se}$</u> | <u>25h</u> | <u>$\pm\text{se}$</u> |
|-----------|-------------|----------------------------------|-------------|----------------------------------|------------|----------------------------------|------------|----------------------------------|
| Glucose | 1.13 | 0.04 | 0.62 | 0.04 | 0.81 | 0.14 | 1.23 | 0.21 |
| Galactose | 0.97 | 0.37 | 0.63 | 0.05 | 1.08 | 0.14 | 0.87 | 0.21 |
| Xylose | 1.22 | 0.50 | 0.48 | 0.13 | 0.94 | 0.20 | 1.12 | 0.39 |
| Rhamnose | 0.66 | 0.12 | 0.68 | 0.22 | 0.88 | 0.17 | 1.26 | 0.26 |

Table 3.4. Monosaccharide concentrations ($\mu\text{g mg}^{-1}$ dry weight) in cell walls of intact muskmelon perisperm tissue determined by HPTLC.

| Sugar | <u>10 h</u> | <u>$\pm\text{se}$</u> | <u>15 h</u> | <u>$\pm\text{se}$</u> | <u>20h</u> | <u>$\pm\text{se}$</u> | <u>25h</u> | <u>$\pm\text{se}$</u> |
|-----------|-------------|----------------------------------|-------------|----------------------------------|------------|----------------------------------|------------|----------------------------------|
| Glucose | 0.92 | 0.09 | 0.80 | 0.28 | 0.68 | 0.14 | 0.88 | 0.13 |
| Galactose | 1.10 | 0.11 | 0.90 | 0.07 | 0.60 | 0.03 | 0.60 | 0.05 |
| Xylose | 1.39 | 0.40 | 1.13 | 0.27 | 0.72 | 0.15 | 0.76 | 0.12 |
| Rhamnose | 1.04 | 0.25 | 0.94 | 0.31 | 0.65 | 0.14 | 1.10 | 0.31 |

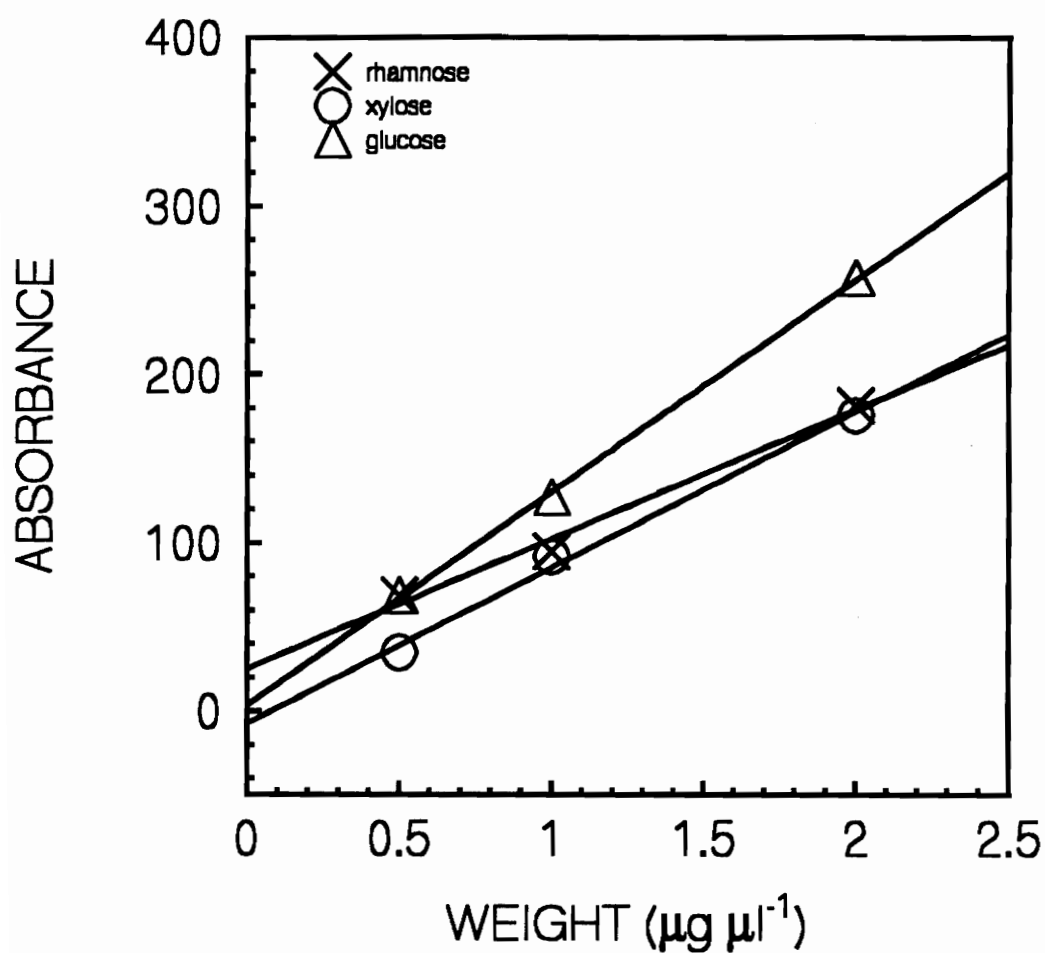


Fig. 3.8. Standard curves for rhamnose, xylose and glucose from HPTLC plates developed with propanol:water (90:10). Visualization: Thymol-sulfuric acid reagent.

The proportion of xylose was high both in the whole perisperm envelope and the perisperm tissue without cone tips (Fig. 3.5 and 3.6). In both cases, all the sugars increased sharply prior to radicle emergence. It is possible that glucuronic acid and galacturonic acids were not detected by HPTLC after acid hydrolysis.

The extra sugars detected by GC possibly resulted from incorrect peak identification. It is possible that the samples were contaminated with embryonic tissue. Since cell wall samples were thoroughly washed in this study, cytoplasmic contamination should have been minimal. The presence of ribose in small amounts has been noted in cell wall preparations of other seeds and was considered to be a cytoplasmic contaminant (Halmer *et al.* 1975). Glucose was present in relatively large amounts in hydrolysates obtained from tomato endosperm and may have originated from both cellulose and possibly from the glucose units in the mannan chains (Groot *et al.* 1988).

These results indicate that mannose is not a component of muskmelon perisperm envelope tissue. This is in contrast to the large amounts of mannose found in the endosperms of lettuce, tomato, and *Datura*, and possibly pepper (Halmer *et al.* 1976, Leung and Bewley 1981, Watkins and Cantliffe 1985, Groot *et al.* 1988, Sanchez *et al.* 1990). It is possible that the difference in cell wall composition of the layers surrounding the embryo could be related to the difference in their structures and origin. Perisperm tissue is maternally derived, whereas endosperm is sexually derived. Galacto-(1→4)- β -mannans are the major reserve carbohydrates in the endosperms of many legumes, including fenugreek, carob, and guar (Dea and Morrison 1975).

Pure mannans are stored in the endosperms of species of Palmae and Umbelliferae (Hopf and Kandler 1977). Galacto-(1→4)-β-glucan-(1→4)-β-mannans are the major reserve carbohydrates in the endosperms of Liliaceae and Iridiaceae (Dea and Morrison 1975). The results presented in this study indicate that the major sugars in muskmelon perisperm envelope are glucose, galactose, xylose, and rhamnose. Polysaccharide components from such monomers could consist of glucans, galactans, galactoxyloglucans, xyloglucans, or possibly xylogalactans (Halmer 1985).

The results obtained by GC and HPTLC portrayed increased sugar concentrations prior to radicle emergence. It is possible that the samples were contaminated with embryonic tissue which caused the apparent increase in sugar concentrations at 25 h. This is contrary to previous work using lettuce, *Datura*, and tomato (Halmer *et al.* 1976, Leung and Bewley 1981, Groot *et al.* 1988, Sanchez *et al.* 1990). In *Datura*, for instance, the mannose content decreased prior to radicle emergence while the rest of the sugars remained relatively stable throughout imbibition. Since mannose is not a component of muskmelon perisperm envelope tissue, the assumption that β-mannanase is not the enzyme involved in perisperm weakening is valid. It appears that (1→4)-β-glucanase or α-galactosidase may be the key enzymes involved in perisperm cell wall degradation. Similar amounts of α-galactosidase exist in both dry and imbibed isolated lettuce endosperm and are responsible for the release of galactose (Reid and Meier 1973, Reid *et al.* 1977, Leung and Bewley 1983, Ouelette and Bewley 1986). It is possible that cellulose and uronic acids might be involved, but these were not tested in the study.

CHAPTER FOUR

CHANGES IN THE STRENGTH OF PERISPERM TISSUE DURING MUSKMELON SEED GERMINATION

INTRODUCTION

Seed coats and surrounding structures may influence the ability of a seed to germinate through interference with water uptake, gas exchange, diffusion of endogenous inhibitors, or by mechanical restriction of embryo growth (Ikuma and Thimann 1963, Mayer and Shain 1974). In seeds that do not have hard seed coats or require scarification for water uptake, other seed parts, such as endosperm or other heterogeneous tissue may mechanically restrict embryo expansion, thus preventing radicle growth and emergence (Georghiou *et al.* 1983, Watkins *et al.* 1985, Sanchez *et al.* 1990, Welbaum and Bradford 1990a). For instance, removal of the endosperm surrounding *Syringa* embryos alleviates dormancy that results from mechanical restriction of radicle emergence (Juntilla 1973).

Encasing the embryo of seeds of lettuce, *Datura*, tomato, pepper, and muskmelon, for example, are maternal tissues such as endosperm, perisperm, or other heterogeneous tissues that may restrict radicle growth (Georghiou *et al.* 1983, Groot and Karssen 1987, Watkins *et al.* 1985, Sanchez *et al.* 1990, Welbaum and Bradford 1990a). In such seeds, the germination process appears to be controlled by weakening of endosperm tissue which frees the embryo from mechanical restraint (Jones 1974, Georghiou *et al.* 1981, Liptay and Schopfer 1983, Groot and Karssen 1987, Sanchez *et al.* 1990, Welbaum

and Bradford 1990b). Several authors have proposed that endosperm weakening could be a mechanical as well as an enzymatic process (Ikuma and Thimann 1963, Pavlista and Haber 1970, Mayer and Shain 1974), controlled by phytochrome activity and growth regulators in some cases (Psaras *et al.* 1981, Watkins and Cantliffe 1983, Groot and Karssen 1987).

The two-cell-layered lettuce endosperm, consisting of thick-walled mannan-rich cells, is a tough, resistant coat which may resist penetration by the expanding radicle. For instance, inhibition of endosperm weakening in lettuce seeds using bleach resulted in embryo growth without endosperm penetration (Pavlista and Haber 1970). The ability of endosperm tissue to control radicle growth in lettuce has been widely debated. Turgor generated by the growing embryo may puncture the endosperm (Nabors and Lang 1971a, 1971b, Carpita *et al.* 1979a, 1979b). Enzymatic weakening of endosperm tissue may be required for germination to occur (Pavlista and Haber 1970, Ikuma and Thimann 1963). A decrease in mechanical strength of lettuce endosperm tissue was measured during germination using an Instron Universal Testing Machine (Tao and Khan 1987). Although the puncture-force required to penetrate the endosperm decreased during imbibition, endosperm strength did not correlate to radicle protrusion. Red-light induced both an increase in growth potential of the lettuce embryonic axes (Nabors and Lang 1971a, 1971b, Carpita *et al.* 1979a, 1979b) and structural changes in the endosperm that coincided with radicle emergence (Jones 1974, Pavlista and Valdovinos 1978, Psaras *et al.* 1981, Georghiou *et al.* 1983, Psaras 1983).

Tomato embryos are surrounded by a non-starchy endosperm that restrains embryo expansion (Haigh and Barlow 1987, Liptay and Schopher 1982, Groot *et al.* 1988). Haigh and Barlow (1987) suggested that tomato seed germination depended on endosperm weakening, because turgor remained constant throughout imbibition. Haigh and Barlow (1990) reported that the tomato embryo was capable of expansive growth, but the endosperm tissue enclosing the embryo restricted the hydration level of the embryo prior to its emergence. Groot and Karssen (1987) used an Instron to determine the puncture-force needed to penetrate the endosperm of imbibed wild-type and gibberellin-deficient mutant tomato seeds. Tomato seed germination depended on gibberellic acid to induce weakening of the layers opposing radicle emergence.

In *Datura*, a seven- to nine- cell-layered endosperm surrounding the embryo acts as a mechanical barrier to the expanding embryo during germination. Endosperm weakening is necessary for *Datura* seed germination (Sanchez *et al.* 1986). Endosperm softening in *Datura ferox* was measured by Force Induced Protrusion (FIP) in an attempt to verify the relationship between phytochrome activity and endosperm weakening. Force Induced Protrusion was determined by applying a force of up to 1200 g on a 3.0 mm² surface placed in the middle of a decoated seed. The radicle protruded out of the endosperm if the section of the tissue in contact with the radicle end was sufficiently softened. The number of red-light induced seeds susceptible to FIP increased with time, while that of far-red-light induced seeds did not change. This analysis showed that endosperm softening was necessary for radicle emergence in *Datura ferox*.

In pepper, the endosperm tissue restricts radicle emergence. Watkins and Cantliffe (1983) measured the mechanical resistance imposed by the endosperm on the radicle using an Instron. Although endosperm strength decreased with imbibition time, seeds imbibed at 25°C required a lower puncture-force than at 15°C. The puncture-force at 25°C decreased with exogenous application of gibberellin. The workers correlated reduction in puncture-force caused by exogenous supply of GA with ability of pepper seeds to germinate.

The perisperm envelope in muskmelon consists of a two- to four- cell-layered perisperm and a single-cell layered endosperm surrounding the embryo. The perisperm mechanically restrains radicle growth during germination (Welbaum and Bradford 1990a). In a previous study, muskmelon embryo turgor remained constant prior to radicle growth (Welbaum and Bradford 1990b). This suggests that weakening of the muskmelon perisperm envelope occurs prior to germination.

The focus of the current study is to clarify the role of the perisperm envelope in muskmelon seed germination by measuring the forces required to penetrate muskmelon perisperm tissue before and after radicle protrusion using an Instron.

MATERIALS AND METHODS

Plant material

Muskmelon (cv. Top Mark) fruits were harvested 50 d after anthesis in 1987. The seeds were stored at 5°C.

Incubation conditions

Twenty seeds were incubated in 9-cm petri dishes on two thickness of germination blotter paper (Anchor Paper Co.) moistened with 10 ml of distilled water. Seeds were incubated at 25°C for 5, 10, 15, 20, 22, 23, and 25 h. Twenty-five seeds were tested from each time interval, and all treatments were replicated twice.

Puncture-test

The Instron Universal Testing Machine (Model, 1123) was used to determine perisperm strength. Seeds were decoated and cut approximately 5 mm below the radicle tip. Each tip was immobilized on a wooden block for the puncture-test. The wooden block was centered on a pressure-sensitive (20 Newton) load cell set at (5 Newton) full scale. A pointed needle (tip diameter, 0.24 mm) was lowered through the center of the seed piece at a crosshead speed of 5 mm min⁻¹. Each test-run was 90 s.

Crosshead speed test

Three crosshead speeds of 1, 5, and 50 mm min⁻¹ were tested in seeds imbibed for 5 and 15 h using the needle described above. Twenty-five seeds from each time interval were tested. The test-runs were 20 s, 90 s, and 6 min, respectively.

Quantification

The force needed to penetrate the perisperm envelope adjacent to the radicle was determined from the peak on the chart recorder graph. The energy needed to penetrate the perisperm was calculated from the area under the curve of the chart recorder graph until the time that the perisperm was punctured. Twenty-five seeds were measured at each time interval, and means were expressed as \pm S.E. Mean values from germinated seeds (25 h) were subtracted from non-germinated seeds to estimate the resistance of the perisperm tissue separately from the other tissues.

RESULTS AND DISCUSSION

Germination timing was similar to that described in the previous studies (Fig. 2.1). Radicle emergence was evident at 23 h after imbibition. By 25 h, germination had occurred in most seeds, as indicated by the significant reduction in mechanical strength of the perisperm tissue. Generally, the force required to penetrate muskmelon perisperm envelope decreased with imbibition time. The 1.50 N puncture-force for dry seeds decreased throughout imbibition to only 0.5 N prior to radicle emergence (Fig. 4.1). The energy required to penetrate the muskmelon perisperm envelope also declined during imbibition (Fig. 4.2). Dry seeds required almost twice as much energy as that needed to puncture germinating seeds. The mechanical resistance of the perisperm envelope to penetration decreased significantly during imbibition, as demonstrated by the steady decrease in energy from 10 to 23 h after imbibition.

The output from the load cell revealed differences in resistance of seed tissues to penetration. Generally, the force increased steadily as the needle penetrated the cotyledons and then dropped as the needle penetrated the embryo. A sharp decrease in force marked puncture of the perisperm envelope in imbibed seeds not showing radicle emergence (Fig. 4.3). In germinated seeds, the force increased gradually as the needle penetrated the cotyledons and the embryonic axis without reaching a peak (Fig. 4.4). The output from dry seeds was variable, because seed pieces were fractured by the needle during the puncture-test.

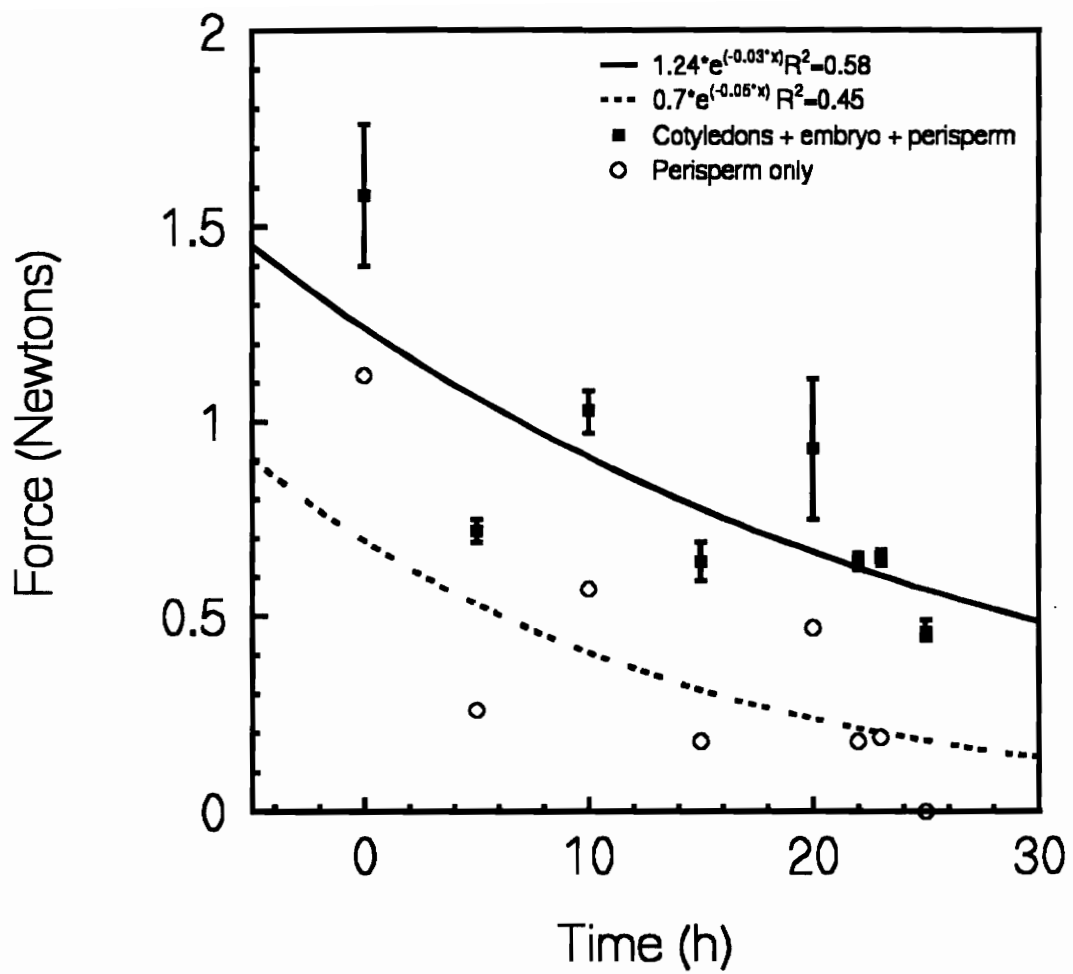


Fig. 4.1. Changes in the force needed to penetrate the muskmelon perisperm tissue during imbibition. Radicle emergence was evident at 23 h.

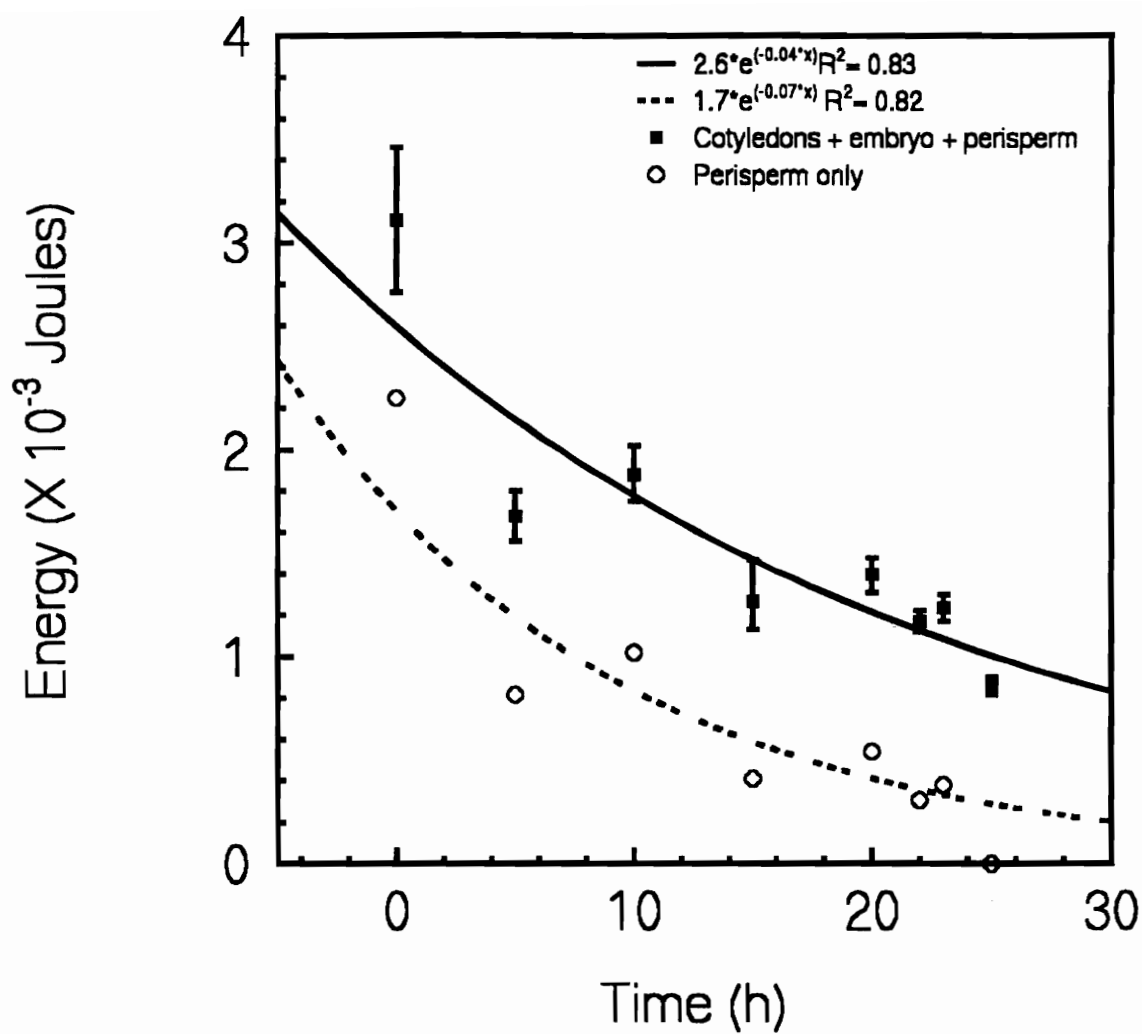


Fig. 4.2. Changes in the energy needed to penetrate the muskmelon perisperm tissue during imbibition. Radicle emergence was evident at 23 h.

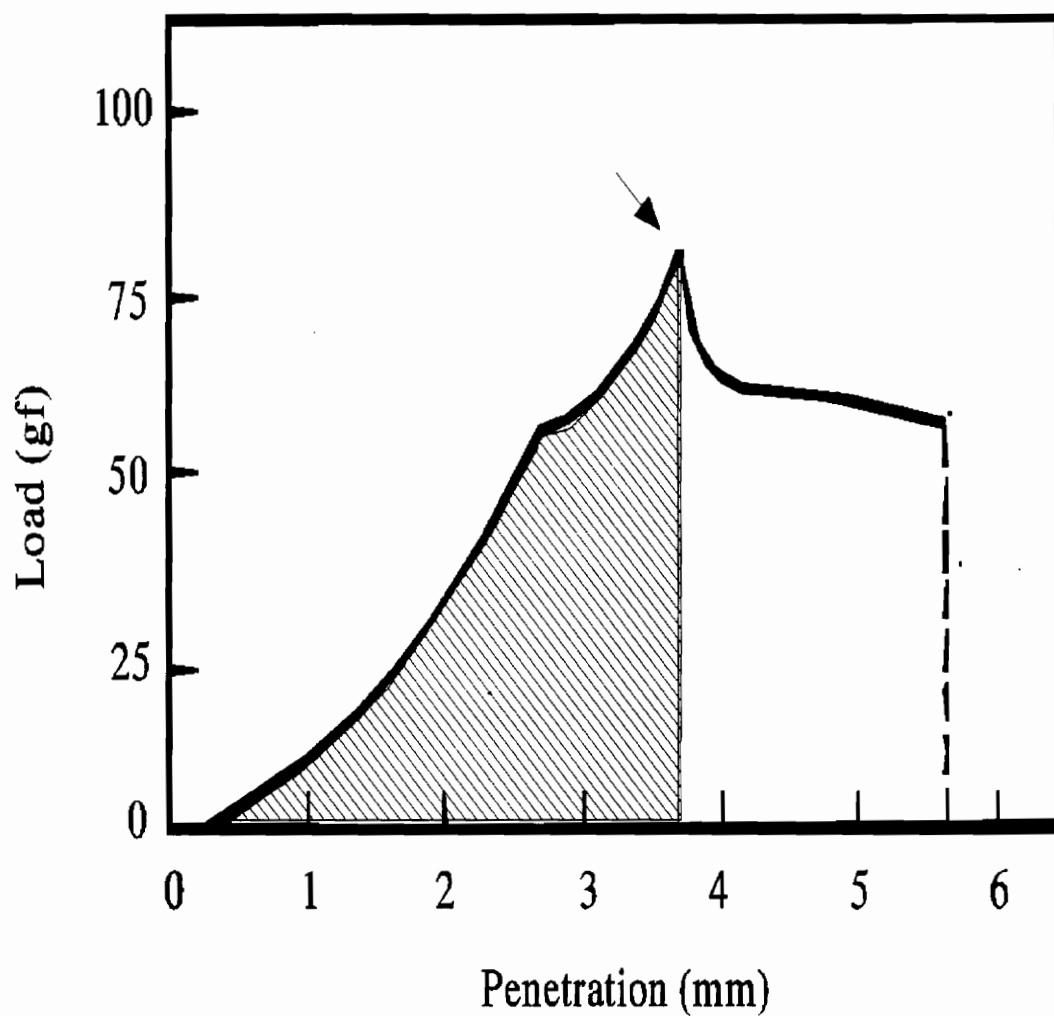


Fig. 4.3. Changes in pressure of the muskmelon seed tissues at 22 h during penetration. The arrow shows the peak (maximum load) and the cross-hatch shows the total energy.

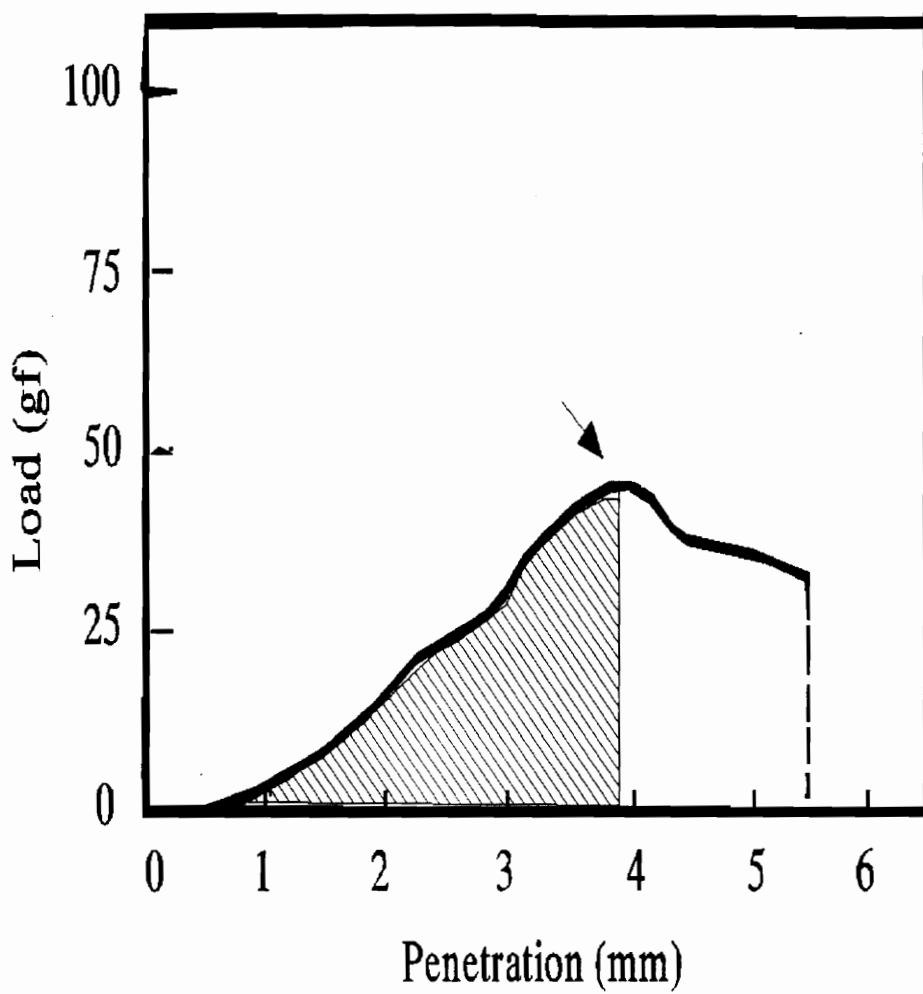


Fig. 4.4. Changes in pressure of the muskmelon seed tissues at 25 h during penetration. The arrow shows the peak (maximum load) and the cross-hatch shows the total energy.

Dry seeds were difficult to puncture, mainly because they were thin and brittle compared to the softer, hydrated seeds.

The influence of crosshead speed on the puncture-test was investigated during the study. A decrease in crosshead speed from 50 to 1 mm min⁻¹ resulted in a decrease in energy (Fig. 4.5) and force (Fig. 4.6) needed to penetrate muskmelon perisperm envelope at 5 and 15 h. The results suggest that above 5 mm min⁻¹ crosshead speed is not a factor, but below 5 mm min⁻¹ the crosshead speed is critical. Out of the three crosshead speeds tested during the study, a crosshead speed of 1 mm min⁻¹ was significantly different from the other two (Fig. 4.5 and 4.6). A crosshead speed below 5 mm min⁻¹ may be closer to the static nature of radicle emergence. The crosshead speed obviously is a critical factor in determining the appropriate puncture-force.

The amount of mechanical restraint varies in different species possibly due to the difference in composition of the layers surrounding the embryo or the method of analysis. The thick cell wall and the dense cytoplasm of the lettuce endosperm cells (Jones 1974) attest to the strength of the endosperm layer. Tao and Khan (1987) estimated the puncture-force needed to penetrate the endosperm of dark-imbibed lettuce seeds using a 5 mm min⁻¹ crosshead speed. Although the puncture-force was 0.6 Newton and 0.4 Newton for seeds exposed to light and GA, respectively, the radicles of seeds treated with the growth regulator were much slower to emerge. Similarly, the puncture-force of wild-type tomato endosperm was estimated at a crosshead speed of 5 mm min⁻¹. The puncture-force decreased from 0.6 N to 0.2 N before radicle emergence.

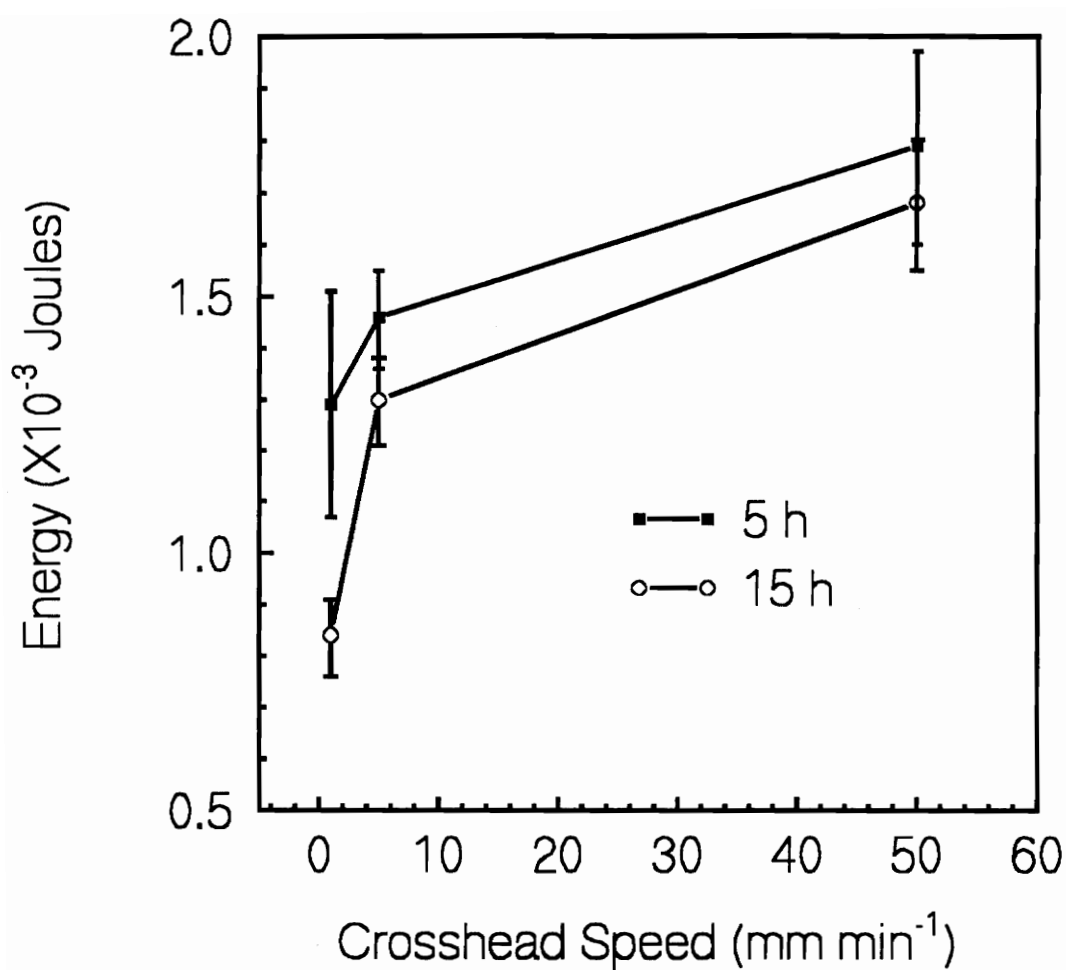


Fig. 4.5. Changes in the energy required to penetrate the muskmelon perisperm envelope tissue using three crosshead speeds.

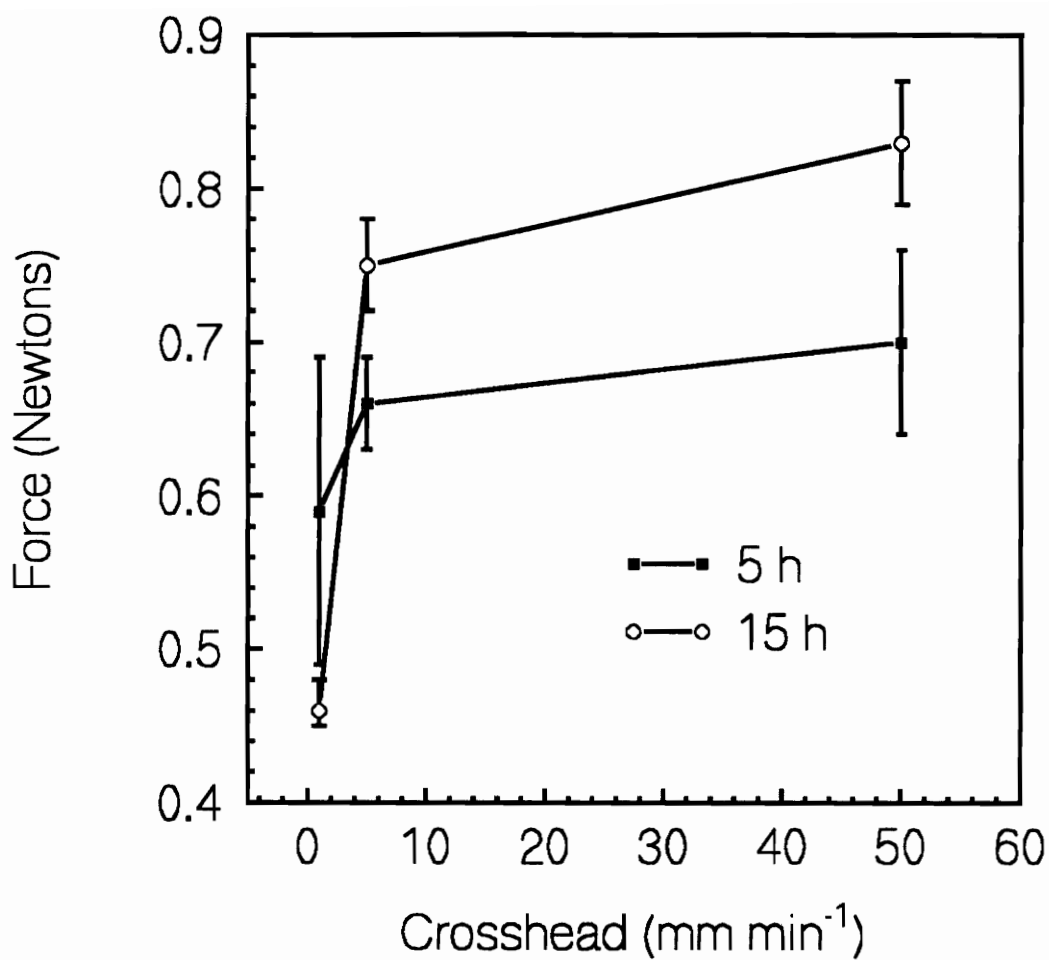


Fig. 4.6. Changes in the force required to penetrate the muskmelon perisperm envelope tissue using three crosshead speeds.

Mechanical strength of the pepper endosperm, estimated at 1.3 mm min^{-1} crosshead speed, decreased from 0.8 N to 0.3 N during imbibition (Watkins and Cantliffe 1987). In *Datura*, a 1200 g (12 N) load applied on the surface of imbibed seeds caused protrusion of the radicle tip through the endosperm, when the section of the tissue in contact with the radicle end was sufficiently softened (Sanchez *et al.* 1986). The strength of *Datura* endosperm may also be similar to lettuce, tomato, and pepper, although a direct comparison is not possible due to the different methods of analysis.

The puncture-test was performed using decoated muskmelon seeds, because the seed coat adjacent to the radicle tip ruptures before radicle emergence. The pepper seed coat does not offer mechanical restriction to the expanding embryo (Watkins and Cantliffe 1987). Tao and Khan (1979) detected changes exclusively in the force required to puncture lettuce endosperm tissue and not intact seeds or pericarp.

Since it was impossible to separate the intact perisperm envelope from the embryo, the values obtained in the current study represent the force and energy required to penetrate the cotyledons, embryonic tissue, and perisperm envelope. If the values from germinated muskmelon seeds are subtracted from each time period, the remainder possibly represents the actual resistance from the perisperm envelope during germination (Fig 4.3 and 4.4).

The current results suggest that muskmelon perisperm envelope mechanically restricts embryo expansion, and weakening of the perisperm envelope is necessary for germination to occur (Welbaum and Bradford 1990a, 1990b). Radicle growth could result from increased embryo turgor, weakening of the perisperm tissue, or a combination of both. In a previous

report, turgor of the embryonic axis did not increase prior to radicle emergence (Welbaum and Bradford 1990a). The reduction in mechanical strength of perisperm envelope of muskmelon seeds during germination is consistent with results obtained using seeds of pepper, tomato, lettuce, and *Datura* (Groot and Karssen 1987, Sanchez *et al.* 1986, Tao and Khan 1987, Watkins and Cantliffe 1987). Tao and Khan (1987) did not observe any changes in puncture-force needed to penetrate isolated embryo, cotyledons, and pericarp of lettuce seeds during imbibition.

Lettuce seeds require a mechanical force from the growing embryo pushing against the endosperm for germination to occur (Pavlista and Haber 1987, Nabors and Lang 1971a, 1971b, Tao and Khan 1987). Red-light alleviates dormancy in lettuce seeds by inducing an increase in embryo growth potential equivalent to 0.31 to 0.38 molar. The force generated is sufficient for the radicle to puncture the endosperm, testa, and pericarp (Nabors and Lang 1971a, Tao and Khan 1987). Although a minimum turgor is required for growth to occur (Lockhart 1965), there is no evidence of embryo turgor build-up in tomato (Haigh and Barlow 1987) and muskmelon (Welbaum and Bradford 1990b) prior to radicle emergence. However, in both cases, embryo water content was limited by 20% and 50%, in tomato, and muskmelon, respectively, because the layers enclosing the embryo mechanically restricted embryo swelling during imbibition. Since both types of seeds were fully hydrated and at zero water potential, a weakening of the endosperm and perisperm was necessary to create a water potential gradient for the additional water uptake needed for expansive growth in these seeds. The results presented in this study support the hypothesis that reduction in

reduction in mechanical strength of muskmelon perisperm envelope is necessary for germination to occur.

SUMMARY

Scanning electron micrographs showed pre-germinative anatomical changes at the micropylar end of muskmelon perisperm envelope prior to radicle protrusion. The structure of the perisperm cone tip cell walls remained unchanged at 10 and 15 h after imbibition. The structural changes evident at 20 h after imbibition were characterized by large fractures between adjacent cells. In some cases, degraded endosperm cells directly opposite the radicle tip appeared crushed and lacked cellular integrity. Extensive degradation was evident in perisperm cone tip cell walls at 25 h, mostly in the area surrounding the radicle tip. Germination was defined as protrusion by the radicle through the perisperm envelope and began between 23 and 25 h after imbibition. The endosperm cells were severely eroded with an obvious loss of cellular contents and wall material at the time of germination. The extent of perisperm degradation was not uniform. In all cases, the cells not in contact with the radicle tip were still intact with no signs of degradation. Localized perisperm degradation could have resulted from enzymatic activity in combination with pressure from the expanding embryo. The results suggest that degradation of perisperm cone tip cell walls prior to radicle protrusion is a key event in muskmelon seed germination. This is in agreement with results obtained by (Psaras *et al.* 1981, Georghiou *et al.* 1983, Psaras 1984, Watkins *et al.* 1985, Haigh and Barlow 1987, Sanchez *et al.* 1990).

Acid hydrolysis of purified perisperm cell walls yielded four monosaccharides. The cone tips contain fairly large amounts of glucose

and galactose and lesser amounts of xylose and rhamnose. The proportion of xylose was higher in the intact perisperm tissue than in the cone tips. In all cases, the sugar concentrations decreased steadily between 10 and 20 h after imbibition and then increased sharply prior to radicle emergence. Contamination from embryonic tissue apparently caused the increase in sugar concentrations at 25 h. Since the perisperm envelope cell wall is largely composed of glucose, galactose, xylose, and rhamnose, the cell wall polysaccharides were possibly glucans, galactans, xyloglucans, or possibly xylogalactans.

Mannose is not a component of the muskmelon perisperm envelope. This is in contrast to the large amounts of mannose found in the endosperms of lettuce, tomato, and *Datura* which have cell walls composed of galactomannans and/or glucomannans (Halmer *et al.* 1976, Leung and Bewley 1981, Groot *et al.* 1988, Sanchez *et al.* 1990). Since mannose is not a component of muskmelon perisperm cell walls, endo- β -mannanase is not likely to be involved in perisperm weakening as is the case in lettuce, tomato, and *Datura* seeds. It appears that (1 \rightarrow 4)- β -glucanase or α -galactosidase may be the key enzymes involved in perisperm cell wall degradation during muskmelon seed germination.

The force and energy required to penetrate the muskmelon perisperm envelope decreased during imbibition. The 1.5 N puncture-force for dry seeds decreased throughout imbibition to only 0.5 N at 25 h. The energy declined from 3×10^{-1} Joules for dry seeds to 1.5×10^{-1} Joules at radicle emergence. These results suggest that the muskmelon perisperm envelope mechanically restricts embryo expansion and that weakening of the perisperm

envelope is necessary for germination to occur. The reduction in mechanical strength of the perisperm envelope of muskmelon seeds during germination is similar to results obtained for pepper, tomato, lettuce, and *Datura* seeds (Sanchez *et al.* 1986, Groot and Karssen 1987, Tao and Khan 1987, Watkins and Cantliffe 1987).

LITERATURE CITED

- Adachi S. 1965. Thin-layer chromatography of carbohydrates in the presence of bisulfite. *J. Chromatogr.* 17: 295-299
- Albersheim P., and Nevins D.J., English P.D., Karr A. 1967. A method for the analysis of sugars in plant cell wall polysaccharides by GLC. *Carbohydr. Res.* 5: 340-345
- Bewley J.D., and Black M. 1982. Physiology and biochemistry of seeds in relation with germination Vol 2. Springer-Verlag, Berlin
- Biermann C.J. 1988. Hydrolysis and other cleavages of glycosidic linkages in polysaccharides. *Advances in carbohydrate chemistry and biochemistry.* 46: 251-271
- Black M., and Chapman J. Topics in plant physiology: 2. Brett C. and Waldron K. Physiology and biochemistry of plant cell walls. p 4-57. unwin Hyman Ltd. 1990
- Bradford J.K. 1990. A water relations analysis of seed germination rates. *Plant Physiol.* 94: 840-849.
- Carpita N.C., and Nabors M.W. 1979. The influence of growth regulators on the growth of embryonic axes of red- and far-red-treated seeds. *Planta* 145: 511-516
- Carpita N.C., Nabors M.W., Ross C.W., and Peteric L. 1979a. The growth physics and water relations of red-light induced germination in lettuce seeds. III. Changes in the osmotic and pressure potential in the embryonic axes of red-and far-red treated seeds. *Planta* 144: 217-224
- Carpita N.C., Nabors M.W., Ross C.W., and Peteric N.L. 1979b. The growth physics and water relations of red-light-induced germination in lettuce seed. IV. Biochemical changes in the embryonic axes of Red- and Far-red-treated seeds. *Planta* 144: 225-233

Courtois J.E., Le Dizet P., and Robic D. 1976. Étude complémentaire de la structure de trois galactoxyloglucanes (amyloïdes) de graines. *Carbohydr. Res.* 49: 439-449

Dahal P., and Bradford K.J. 1990. Effects of priming and endosperm integrity on seed germination rates of tomato genotypes. II. Germination at reduced water potential. *J. Exp. Bot.* 41: 1414-1453

Dea I.C.M., and Morrison A. 1975. Chemistry and interactions of seed galactomannans. *Adv. Carbohydr. Chem. Biochem.* 31: 241-312

Dulson J., Bewley J.D., and Johnson R.N. 1988. Abscissic acid is an endogenous inhibitor in the regulation of mannanase production by isolated lettuce (*Lactuca sativa* cv. Grand Rapids) endosperms. *Plant Physiol.* 87: 660-665

Evenari M. Light and seed dormancy. In *Encycl. Plant Physiol.*, vol. XV, pt. 2, 808-847, ed. A. Lang. Berlin-Heidelberg New York: Springer 1965

Fell R. D. 1990. The qualitative and quantitative analysis of insect hemolymph sugars by high performance thin-layer chromatography. *Comp. Biochem. Physiol.* 95: 539-544.

Georghiou K., Psaras G., and Mitrakos K. 1983. Lettuce endosperm structural changes during germination under different light, temperature, and hydration conditions. *Bot. Gaz.* 144: 207-211

Ghebregzabher M., Rufini S., Monaldi B., and Lato M. 1976. Thin-layer chromatography of carbohydrates. *J. Chromatogr.* 127: 133-162.

Groot S.P.C., and Karssen C.M. 1987. Gibberellins regulate seed germination in tomato by endosperm weakening: a study with GA-deficient mutants. *Planta* 171: 525-531

Groot S.P.C., Kieliszewaska-Rokicha B., Vermeer E., and Karssen C.M. 1988. Gibberellin-induced hydrolysis of endosperm cell walls in gibberellin-deficient tomato seeds prior to radicle protrusion. *Planta* 174: 500-504

Halmer P. 1985. The mobilization of storage carbohydrates in germinated seeds. *Physiol. Vég.* 23: 107-125

Halmer P., Bewley J.D., and Thorpe T.A. 1976. An enzyme to degrade lettuce endosperm cell walls. Appearance of a mannanase following phytochrome- and gibberellin-induced germination. *Planta* 130: 189-196

Halmer P., and Bewley J.D. 1979. Mannanase production by the lettuce endosperm. Control by the embryo. *Planta* 144: 333-340

Halmer P., Bewley J.D., and Thorpe T.A. 1975. Enzyme to break down lettuce endosperm cell wall during gibberellin- and light- induced germination. *Nature* 258: 716-718

Haigh A.M., and Barlow E.W.R. 1987. Water relations of tomato seed germination. *Aust. J. Plant. Physiol.* 14: 485-492

Haigh A.M., Groot S.P.C., Zingen-Sell I., and Karssen C.M. The role of endosperm degradation in the germination of tomato seeds. NATO ASI Series, Vol. H35. Cell Separation in Plants. Springer-Verlag Berlin Heidelberg 1989

Hopf H., and Kandler O. 1977. Characterization of the reserve cellulose of the endosperm of as a $\beta(1\rightarrow4)$ mannan. *Phytochemistry* 16: 1715-1717

John F.R., and Bernard J.L. Biochemical techniques: Theory and Practice. White Iowa State University. Brooks/Cole Publishing Co. Monterey, California 1987

- Jones R.L. 1974. The structure of lettuce endosperm. *Planta* 121: 133-146
- Jacobsen J.V., Pressman E., and Pylotis N.A. 1976. Gibberellic induced separation of cells in the isolated endosperm of celery seed. *Planta* 129: 113-122
- Jacobsen J.V. The seed: germination In Johri B.M. ed. Embryology of angiosperms. Springer-Verlag Berlin Heidelberg New York Tokyo, 1984
- Juntilla O. 1973. The mechanism of low temperature dormancy in mature seeds of *Syringa* species. *Physiol. Plant.* 29: 56-263
- Kartnig T., and Wegschaider O. 1971. Eine Möglichkeit zur Identifizierung von Zuckern aus Kleinsten Mengen von Glykosiden oder aus Zuckergemischen. *J. Chromatogr.* 61: 375-377
- Lee K.Y., Nurok D., and Zlakis A. 1979. Determination of glucose , fructose and sucrose in molasses by high-performance thin-layer chromatography. *J. Chromatogr.* 174: 187-193
- Lenkey B., Çsanyi J., and Nanasi P. 1986. A rapid determination of sucrose and fructose in biological samples by video densiometry. *J. Liq. Chromatogr.* 9: 1869-1875
- Leung D.W.M., and Bewley J.D. 1983. A role for α -galactosidase in the degradation of endosperm cell walls of lettuce seeds, cv. Grand Rapids. *Planta* 157: 274-277
- Liptay A., and Schopfer P. 1983. Effect of water stress, seed coat restraint, and abscisic acid upon different germination capabilities of two tomato lines at low temperature. *Plant Physiol.* 73: 935-938
- Lockhart J.A. 1965. Analysis of irreversible cell elongation. *J. Theor. Biol.* 8: 264-275

- Manzi A.E., Ancibor E., and Cerezo A.S. 1990. Cell wall carbohydrates of the endosperm of the seed of *Gleditsia triacanthos*. *Plant Physiol.* 92: 931-938
- Mahran G.H., El-Fishawy A.M., Hosny A.M.S., and Hilal A.M. 1991. Photochemical and antimicrobial study of *Jacaranda mimosaeifolia* D. Don. grown in Egypt. *Herba Hungarica* 30: 98-104
- Matheson N.K. The synthesis of reserve oligosaccharides and polysaccharides in seeds. Murray, D.R., ed. Academic Press, North Ryde, Australia. In. Seed physiology, vol., 1: Development, pp 167-208, 1984
- Matheson N.K., and Saini H.S. 1977. Polysaccharide and oligosaccharide changes in Lupin cotyledons. *Phytochemistry* 16: 59-66
- Mayer A.M., and Shain Y. 1974. Control of seed germination. *Annu. Rev. Plant Physiol.* 25: 167-193
- McCleary B.V. 1983. Enzymatic interactions in the hydrolysis of galactomannan in germinating guar: The role of exo- β -mannanase. *Phytochemistry* 22: 649-658
- Meier H., and Reid J.S.G. Reserve polysaccharides other than starch in higher plants . In: Encyclopedia of plant physiology, N.S., vol. 13 A: Plant carbohydrates I, pp. 418-471, Loewus, F.A., Tanner, W., eds. Springer, Berlin Heidelberg New York 1982
- Nabors M.W., and Anton L. 1971a. The growth physics and water relations of red-light-induced germination in lettuce seeds. I. Embryos germinating in osmoticum. *Planta* 101: 1-25

Nabors M.W., and Anton L. 1971b The growth physics and water relations of red-light-induced germination in lettuce seeds. II. Embryos germinating in water. *Planta* 101: 26-34

Ni B.R., and Bradford K.J. 1992. Quantitative models characterizing seed germination responses to abscissic acid and osmoticum. *Plant Physiol.* 98: 1057-1068

Ouelette F.F., and Bewley J.D. 1986. β -Mannosidase mannohydrolase and the mobilization of the endosperm cell wall of lettuce seeds, cv. Grand Rapids. *Planta* 169: 333-338

Park W.M., and Chen S.S.C. 1974. Patterns of food utilization by the germinating lettuce seed. *Plant Physiol.* 53: 64-66

Pavlista A.D., and Haber A.H. 1970. Embryo expansion without protrusion in lettuce seeds. *Plant Physiol.* 46: 636-637

Pavlista A.D., and Valdovinos J.G. 1978. Changes in the surface appearance of the endosperm during lettuce achene germination. *Bot. Gaz.* 139: 171-179

Poole C.F., Coddens M.E., Buttler G.T., Schuette S.A., Ho S.S.J., Khatib S., Piet L., and Brown K.K. 1985. Some quantitative aspects of scanning densitometry in high-performance thin-layer chromatography. *J. Liquid Chromatogr.* 8: 2875-2926

Pruden B.B., Pinneault G., and Loufti H. 1975. A thin-layer chromatographic method for quantitative determination of D-mannose, D-glucose and D-galactose in aqueous solution. *J. Chromatogr.* 5: 477-483

Psaras G., Georghiou K., and Mitrakos K. 1981. Red-light-induced endosperm preparation for radicle protrusion of lettuce embryos. *Bot. Gaz.* 142: 13-18

Psaras G., and Georghiou K. 1983. Gibberellic acid-induced structural alterations in the endosperm of germinating *Lactuca sativa* L. achenes.

Zpflanzenphysiol. Bd. 112:15-19

Psaras G. 1984. On the structure of lettuce *Lactuca sativa* L. endosperm during germination. *Ann. Bot.* 54: 187-194

Reid J.S.G., and Meier H. 1972. The function of the aleurone in layer during galactomannan mobilization in germinating seeds of fenugreek (*Trigonella foenum-graecum* L.), crimson clover (*Trifolium incarnatum* L.) and lucerne (*Medicago sativa* L.): a correlative biochemical and ultrastructural study. *Planta* 133: 219-222

Reid J.S.G., Davies C., and Meier H. 1977. Endo- β -mannanase, the leguminous aleurone layer and the storage galactomannan in germinating seeds of *Trigonella foenum-graecum* L. *Planta* 133: 219-222

Sanchez R.A., De Miguel L., and Mercuri O. 1986. Phytochrome control of cellulase activity in *Datura ferox* L. seeds and its relationship with germination. *J. Expt. Bot.* 37: 1574-1580

Sanchez R.A., Sunnel L.A., Labavich J.M., and Bonner B.A. 1990. Changes in the micropylar region of the endosperm, before radicle protrusion in the seeds of two *Datura* species. *Plant Physiol.* 83: 90-118

Schopfer P., Bajracharya D., and Plachy C. 1979. Control of seed germination by abscisic acid. I. Time course of action in *Sinapsis Alba* L. *Plant Physiol.* 64: 822-827

Schopfer P., and Plachy C. 1984. Control of seed germination by abscisic acid. II. Effect on embryo water uptake in *Brassica napus* L. *Plant Physiol.* 79: 155-160

Schopfer P., and Plachy C. 1985. Control of seed germination by abscisic acid. III. Effect on embryo growth (minimum turgor pressure)

and growth coefficient (cell wall extensibility) in *Brassica napus* L. *Plant Physiol.* 76: 676-686

Speer H.L. 1974. Some aspects of the function of the endosperm during germination of lettuce seeds. *Can. J. Bot.* 52: 1117-1121

Sporopoulos G., and Reid J.S.G. 1985. Regulation of α -galactosidase activity and the hydrolysis of galactomannan in the endosperm of fenugreek (*Trigonella foenum-graecum* L) seed. *Planta* 166: 271-275

Takeba G. 1980. Accumulation of free amino acids in the tips of non-thermodormant embryonic axes accounts for the increase in growth potential of New York lettuce seeds. *Plant Cell Physiol.* 21: 1639-1644

Takeba G., and Matsubara S. 1979. Measurement of growth potential of the embryo in New York lettuce seed under various combinations of temperature, red-light, and hormones. *Plant Cell Physiol.* 20: 51-56

Tao K., and Khan A.A. 1979. Changes in the strength of the endosperm during germination. *Plant Physiol.* 63: 126-128

Thanos C. 1984. Phytochrome-mediated accumulation of free amino acids in radicles of germinating water melon seeds. *Plant Physiol.* 60: 126-128

Watkins J.T., and Cantliffe D.J. 1983. Mechanical resistance of the seed coat and endosperm during germination of *Capsicum annum* at low temperature. *Plant Physiol.* 72: 146-150

Watkins J.T., Cantliffe D.J., Haber D.J., and Nell T.A. 1985. Gibberellic acid stimulated degradation of endosperm in pepper. *J. Am. Soc. Hort. Sci.* 110: 61-65

Weges R. 1987. Physiological analysis of methods to relieve dormancy of lettuce seeds. Ph.D. dissertation. Agricultural University. Wageningen. The Netherlands.

Welbaum G.E., and Bradford K.J. 1990a. Water relations of seed development and germination in muskmelon (*Cucumis melo* L.). IV. Characteristics of the perisperm during seed development. *Plant Physiol.* 92: 1038-1045

Welbaum G.E., and Bradford K.J. 1990b. Water relations of seed development and germination in muskmelon (*Cucumis melo* L.). V. Water relations of imbibition and germination. *Plant Physiol.* 92: 1046-1052

York S.W., Darvill A.G., Mcneil M, Stevenson T.T., and Albersheim P. 1986. Methods in Enzymology. *Plant Molecular Biology* 118: 29-32

VITA

Joyce Wangechi Muthui was born on January 8th 1967 in Nairobi, Kenya. She attended Nyeri Primary School and thereafter proceeded to Loreto High School, Limuru in 1980. She pursued a Bachelor of Science degree in Horticulture at Egerton University, Njoro and graduated with honors in 1990. Presently, the author is pursuing a Master of Science degree in Horticulture at Virginia Tech.

A handwritten signature in black ink that reads "Joyce Wangechi Muthui". The script is cursive and fluid, with the first letters of each name being capitalized and prominent.